

REVIEW OF THE MECHANICAL PROPERTIES OF CAST STEELS
WITH EMPHASIS ON FATIGUE BEHAVIOR AND
THE INFLUENCE OF MICRODISCONTINUITIES

by

M. R. Mitchell
Department of Theoretical and Applied Mechanics

ABSTRACT

Mechanical properties of cast steels are dependent on the microdiscontinuities which they inherently contain. Although at lower hardnesses the strength of steel castings may not be significantly altered by microdiscontinuities, their ductilities and impact resistance can be drastically reduced.

In a similar way, the fatigue behavior of cast steels is pronouncely altered by the size, shape and distribution of microdiscontinuities. A proposed course for future research on cast irons in general in which a means of predicting their fatigue behavior accounting for variations in matrix strength and the morphology of the microdiscontinuities is presented.

A Report of the
FRACTURE CONTROL PROGRAM

College of Engineering, University of Illinois
Urbana, Illinois 61801
June, 1975

ACKNOWLEDGMENTS

Technical discussions, criticisms and manuscript reviews and encouragements of Professor JoDean Morrow, University of Illinois, and Dr. R. W. Landgraf, Ford Motor Company, were extremely helpful and are affably acknowledged. Mrs. Darlene Mathine patiently typed the manuscript while Mr. B. D. Agrawal aided in the literature search and prepared the figures for this report.

Introduction

Cast steels are generally considered mechanically inferior to wrought steel products due to the inherent microdiscontinuities* which they contain. However, because of economic considerations and ease of fabricating complex geometries, cast steels enjoy a prominent role in today's foundry industry. Many products, such as locomotive frames, turbine shells, large gears for heavy earthmoving equipment, etc., are made of cast steel, not by choice, but because they cannot be economically or readily made by other fabrication techniques.

Melting processes and foundry practice for cast steels are quite similar to those for the wrought products. The main difference in the cast products is that they require greater amounts of deoxidizers in order to produce sound castings. It is for this reason that the silicon and manganese content is generally higher than a wrought steel of comparable carbon content.

Herein lies the problem, for it is the melting and casting practice which produces the origin, modes of formation, as well as the characteristics of the nonmetallic inclusions and voids in cast steels. Further, it is the size, shape and distribution of these microdiscontinuities which governs the mechanical response of cast steels and ultimately the response of wrought steels** which have their beginnings in the cast ingot.

It is the intent of this report to review the available literature and to summarize research on the fatigue behavior of cast steels with particular emphasis on the influence of internal microdiscontinuities.

*Microdiscontinuities will be used herein to mean inclusions, porosities, blow-holes, internal defects, voids, etc.

**Particularly those of high hardness.

Source of Microdiscontinuity

Sims⁽¹⁾ conveniently defines the nonmetallic inclusions in cast steels as exogenous; those formed by mechanical entrainment or heterogeneous reactions which have their principal source in ladle refractories and endogenous; those resulting from homogeneous reactions and formed mainly during solidification of the molten metal.

Endogenous inclusions are comprised principally of oxides and sulfides. The origin of the oxides being principally from deoxidizing reactions due to additions made at the end of a heat, such as manganese and aluminum, while the origin of sulfide inclusions is dependent on the content and solid solubility of sulfur in the melt as well as the cooling rate of the casting.

Exogenous inclusions, on the other hand, are most prolifically obtained from chemical erosion of ladle refractories. Ablation of furnace slag, particularly acidic, and direct reaction between acid refractories and the manganese in molten steel are the two major sources for silica type exogenous inclusions.

Although not considered inclusions per se, gas pores, microshrinkage, cavities, etc., will be included in this paper as microdiscontinuities. Gas porosities, in general, are the result of solidification processes. When the molten steel begins to solidify (which occurs over a temperature range), the solubility of dissolved gases decreases and they are subsequently rejected. Gases evolving from what is still partially liquid and partially solid are trapped at solid-liquid interfaces (i. e. dendrite arms).

In wrought steel products, which are generally hot worked from the ingot stage, internal gas porosities with interfaces free of oxide coatings will "weld" shut. Cast products, on the other hand, receive no subsequent working and gas porosities generated during solidification are an integral result.

Size

Inclusion size depends primarily on the solidification rate of the casting. An example of Si O_2 inclusions in an ingot of electrolytic iron to which 0.5 w/o Si was added is shown in Fig. 1⁽²⁾. Near the center of a slow-cooled ingot, Si O_2 inclusions of the size shown in Fig. 1a were found. Figure 1b demonstrates a definite size decrease of these inclusions resulting from chill casting of the same melt. Similar examples of the effect of cooling rate on the common inclusions in cast steels (i.e. sulfides, oxides, silicates, etc.) can be found in Refs. 1 and 3 for the interested reader.

Flemings⁽⁴⁾ maintains that these solidification phenomena are strongly dependent on heterogeneous dendrite nucleation and multiplication during cooling processes. For minimum inclusion size it is therefore desirable, from a foundryman's standpoint, to strive for minimal solidification time. This will minimize dendritic arm spacing which is solely dependent on the cooling rate. Secondly, dendrite multiplication during the latter stages of solidification may be accelerated by agitation of the partially solid melt. In this way, primary and secondary dendrite arms are broken preventing coarsening and thereby allowing additional sites for primary dendrites to form. The spacing on these primary arms is much finer than those formed during coarsening and the finished casting will therefore be of superior quality from an inclusion and void standpoint.

Shape

Vast arrays in the shape of inclusions in cast steels are, of course, possible. Examples attesting to this are shown in Fig. 2. For convenience, however, the common sulfide and silicate inclusions are generally designated as Type I, II and III, as shown in Fig. 3.

Silicate inclusions are generally spherical in shape. Sulfide inclusions, however, can undergo a drastic morphological change, which is dependent on the amount of aluminum added to the melt generally as a deoxidizing agent^(3, 5, 6). Figure 4a shows an example of a medium carbon cast steel (0.28 w/o C) with no addition of aluminum. The inclusions consist of globular silicates and Type I sulfides. With the addition of 0.015 w/o Al to the same heat, the inclusions consist of globular sulfides and slightly modified silicates, Fig. 4b. Increasing the aluminum content to 0.025 w/o, as in Fig. 4c, produces no silicate inclusions and only eutectic, Type II, sulfides. Finally, addition of 0.05 w/o Al results in duplex sulfides or Type III inclusions⁽⁵⁾. Of greater importance when the morphological change from globular sulfides to Type II occurs, is that their relative location in the microstructure also changes. The precipitation of the Type II sulfide eutectic is generally confined to narrow grain boundaries thus forming a network. Similar eutectic networks of sulfide inclusions have been reported for cast steels deoxidized with titanium⁽⁷⁾ and zirconium⁽⁸⁾. This phenomenon will be shown in a later section of this paper to have a pronounced degenerative effect on the mechanical properties of cast steels.

Distribution

Since endogenous inclusions are the result of homogeneous reactions in the cast steel melt, there is some element of time involved in order to achieve equilibrium. Given sufficient time, some of the reaction products would float out. Nonetheless, because of the time element and the way in which these inclusions form, they are somewhat uniformly dispersed on a macroscopic scale.

Turkdogan and Grange⁽⁹⁾ illustrate, however, that for initial levels of silicon, manganese and oxygen in a cast steel, there is a carbon level above which gas porosities or blowholes occur resulting from ebullition of carbon monoxide. Such

phenomena can lead to gross void segregations and nonuniform dispersions.

Figure 6a shows an example of 4 x 4 x 18 in - 100 lb ingots containing ~ 0.5 w/o Mn, 70 - 120 ppm O₂, 0.01 - 0.04 w/o Si and 0.03 - 0.10 w/o C⁽¹⁰⁾. As illustrated by the unetched cross sections at the top of the figure, for a fixed manganese content of approximately 0.5 w/o and O₂ concentration of approximately 70 - 120 ppm, varying carbon and silicon contents may or may not result in blowholes. Figure 6b shows a theoretically calculated "band" for Si and C levels above which blowhole formation does not occur and below which it will occur. Results⁽⁹⁾ for higher carbon and silicon contents are shown in Fig. 7. It should be noted that the silicon levels shown in this figure are far below those common for steel castings, however, some high strength low alloy wrought steels have compositions near the "blowhole" region.

On a microscopic scale microdiscontinuities are randomly dispersed. Entire books have been written on this subject and no attempt will be made here to elaborate further. The interested reader is referred to Ref. 11 for additional information.

Mechanical Properties

Classification and Specification

Cast steels are generally classified in four groups according to their carbon or alloy content:

- (1) Low carbon with < 0.20 w/o C
- (2) Medium carbon with 0.20 - 0.50 w/o C
- (3) High carbon with > 0.50 w/o C
- (4) Low alloy in which the total alloy content is < 8 w/o.

Other types of steel castings are also available, such as heat-resistant, corrosion-resistant and austenitic manganese steels, but attention will be focused here on the more common varieties.

Most commonly selected grades of steel castings in the low to medium carbon variety correspond to (1) ASTM* 27 class 65 - 35 (65 ksi ultimate, 35 ksi yield strength), QQ-S-681 Class 2** or SAE 0030*** and (2) high strength castings which are often alloyed, fully heat treated or both, similar to ASTM 148 Class 105 - 85, QQ-S-681 Class 4 C2 or SAE 0105.

Other common ASTM designations for cast steels are ASTM A 216 - fusion-weldable carbon steels for high temperature service, A 217 - ferritic alloy steels for pressure vessels subjected to high temperature and corrosion, A 352 - ferritic steels for pressure vessels for low temperature service and A 356 - ferritic carbon and low alloy steels for heavy walled castings such as steam turbines^(12, 13). A summary of these and other steel casting specifications are shown in Table I⁽¹⁴⁾.

As with wrought products, cast steels may be fully annealed, normalized, quenched and tempered, carburized, etc. Often, to insure minimum hardness in critical sections, hardenability may also be specified.

Typical ranges of mechanical properties under these specifications, depending on composition and microstructure, are:

Ultimate strength (ksi)	60 - 260
Yield strength (ksi)	30 - 210
% Reduction in area	65 - 6
Brinnell hardness	120 - 700

A particular advantage of cast steels is that their mechanical properties do not vary greatly with respect to direction. In this way they are unlike their wrought counterpart. However, as will be shown, the morphology of microdiscontinuities

*ASTM - American Society for Testing Materials

**QQ - Federal Army Ordinance

***SAE - Society of Automotive Engineers

may have a pronounced effect on monotonic stress-strain properties, impact resistance (viz-a-viz fracture toughness), and fatigue behavior.

Strength

Handbooks and similar publications⁽¹²⁻¹⁵⁾ generally state that cast, wrought, rolled or forged steels of comparable hardness and hardenability will have approximately the same tensile and yield strength and ductilities.* The longitudinal properties of rolled or forged steels are somewhat greater than those of equivalent castings, but the transverse properties are lower by an amount proportional to the degree of prior working. As a consequence, when service conditions impose multidirectional loading, the nondirectional characteristics of castings may be an advantage.

Mechanical properties for cast steels are often obtained from machined test bars or coupons cast as part of the casting or cast separately from the same melt. Since (1) cooling rate and foundry practice have been shown to markedly influence the microstructure of castings and (2) there is a mass effect shown in Fig. 8⁽¹²⁾ (common in most ferrous-based castings), it is a rash presumption to assume that such test coupons adequately reflect the mechanical properties of the cast product. For these reasons, it is advantageous to remove test bars from critical areas of castings where minimum specifications must be obtained.

Effect of Carbon

Figure 9 summarizes the combined effect of carbon content and commonly used heat treatments for low, medium and high carbon cast steels⁽¹³⁾. As is common in comparable wrought steels, increasing carbon content increases strength but decreases ductility. Unfortunately, for an adequate comparative basis, Brinnell

*Excluding directionality in the wrought, rolled and forged products.

hardnesses corresponding to the specified heat treatments shown on the figure are not given. It is reasonable that the curve of tensile strength for the water quenched and tempered at 1200° F condition would be above that for the annealed condition strictly as a result of presumed hardness differences (annealed being less hard). Reduction in areas would appear at first to be inconsistent with the above reasoning (i.e. annealed being less ductile for equal carbon contents). It is possible that a difference in grain size exists depending on the austenitizing or annealing temperature as illustrated in Fig. 10. Sinclair and Dolan⁽¹⁶⁾ have illustrated for cases in which the microstructure was essentially pearlitic, an increase in prior austenitic grain size reduced ductility when compared to tempered martensitic structures. Also, the annealed samples in Fig. 9 would more closely approach an equilibrium cooled structure in which the iron carbide would precipitate as lamellae (pearlite), while the water quenched and tempered structure would have essentially spherical carbides. Similar reasoning can also be applied to the juxtaposition of the ductility curves for the normalized (part lamella, part spheroidal carbide) and normalized and tempered (essentially spheroidal carbide). From simply a localized plastic constraint standpoint, the pearlitic structure should be less ductile.

Hardness

Ultimate strength in ksi of wrought steels is often approximated by taking one-half the BHN as shown in Fig. 11^(17, 18). Superimposed on this figure are data for cast steels^(18, 19). Results for the wrought steels are closely approximated by this relation except at fairly high hardness (i.e. greater than approximately 500 BHN⁽²⁰⁾) where the influence of inclusions is prominent. Cast steels also follow this relation but appear to deviate at lower hardnesses (i.e. approximately 300 BHN). Observations made by McKenzie⁽²¹⁾ for gray cast iron show

the UTS-BHN relation is totally inappropriate while Testin⁽²²⁾ noted that if the ultimate strength is corrected for net cross sectional area ($\sim 10\%$), the relation was applicable to nodular iron data for hardnesses to approximately 450 BHN.

Such a simplistic view does not appear applicable in the case of the cast steels. Unlike nodular irons in which the area fraction occupied by graphite may range between 6 to 14%⁽²³⁾ with an average of approximately 10%, the microdiscontinuities in cast steels occupy approximately 0.5%⁽²⁴⁾ of the area. What seems more appropriate is the influence of shape on the theoretical stress concentrating effect of the "second phase" particles.

If Type II sulfides in cast steels are approximated as ellipses⁽²⁵⁾ as shown in Fig. 12, the theoretical stress concentration factor, K_t , for a two-dimensional condition and axial loading is:

$$K_t = 1 + \frac{2a}{b}$$

$$r = \frac{b^2}{a}$$

$$\therefore K_t = 1 + 2\sqrt{\frac{a}{r}}$$

where;

a = semi-major axis

b = semi-minor axis

r = tip radius

with an ellipticity of four ($a = 4b$), $K_t = 9$. For the case of nodular iron, the graphite is approximated with $b = a$; $K_t = 3$. Presuming that plastic blunting of the nodules and Type II inclusions occur under an applied load, as illustrated in Fig. 13, the stress concentrating effect of the nodule will decrease ($r \longrightarrow \infty$) and approach unity (Fig. 13a), whereas that of the ellipse (Fig. 13b) will decrease but still have a value greater than one. The degree of blunting is a function of matrix hardness in both instances and, thus, the lower threshold value of the UTS-BHN relation for cast steels, since the shape of the inclusions are markedly different.

Ductility

Inclusion shape is also responsible for drastic reductions in ductility of cast steels^(1, 3, 5, 6). As mentioned in a previous section of this report, the addition of aluminum to cast steels affects the morphological features of sulfides. To illustrate this, Table 2⁽³⁾ lists tensile and impact test results for a medium carbon steel, with and without aluminum, cast in a variety of mold materials. Ultimate strengths are approximately the same, however, ductilities of the cast steel with aluminum additions are consistently lower than without the aluminum.

Table 3⁽⁵⁾ shows the effect of increasing the manganese and sulfur content of a melt deoxidized with 0.05 w/o Al. Increasing sulfur contents progressively lowers the ductilities and impact resistance without appreciable changes in strength. Increasing manganese content increases both the yield and ultimate strength but has little effect on ductility.

The effect of aluminum and sulfur are shown in Table 4⁽⁵⁾. Clearly, with other conditions essentially constant, addition of increments of aluminum to this medium carbon cast steel produces an initial decrease in ductility and impact resistance. Minimum values are then reached and further increases of aluminum cause a recovery of ductility and impact resistance. Figure 14 shows the quantitative effect of these additions. Additions of up to 0.25 w/o Al result in an almost full recovery of the initial, "aluminum free" ductility. Even with no aluminum, the ductility and impact resistance vary inversely with sulfur content as shown in Fig. 15.

Figure 4 reveals that the shape characteristics of the sulfide inclusions is drastically altered because of the addition of certain weight fractions of aluminum. In all cases cited above, the lowest ductilities and impact resistances are invariably attributable to Type II sulfide inclusions.

Occurrence of what is called intergranular fracture or "rock candy" fracture⁽²⁶⁻²⁹⁾ has been directly traced to "chains of non-metallic particles" in cast steels. Originally

thought to be caused by Type II sulfide inclusions, these networks were later shown to be aluminum nitride precipitates at primary austenite grain boundaries. A definite correlation was noted between the percent intergranular fracture of impact specimens and the amount of aluminum added. Increasing the aluminum resulted in increased percentages of intergranular fracture. Generally the aluminum content of the cast steels was in excess of what would cause Type II inclusions and, as shown in Fig. 16, excess nitrogen in conjunction with aluminum to form AlN precipitates in the grain boundaries was the main contributor to the fracture behavior⁽²⁸⁾. This phenomena can be avoided by deoxidizing with titanium, zirconium or titanium-aluminum combinations⁽²⁷⁾.

Fatigue Properties

As indicated in the previous section, the properties of cast steels may be improved substantially by controlling the nature (size and shape) of non-metallic inclusions, voids, pores, etc. In this section the fatigue behavior of cast steels will be reviewed with, again, particular emphasis to the influence of microdiscontinuities.

A compendium of the fatigue behavior of cast steels and comparable wrought steels is presented by Evans, et al.⁽¹⁹⁾. Variables influencing the fatigue resistance of cast steels which were investigated include (1) composition and heat treatment, (2) surface finish, (3) directionality and (4) section size.

Composition and Heat Treatment

Effects of composition and heat treatment on the fatigue properties of cast steels are generally attributed to alteration of the tensile strength^(12, 13, 30, 31). Table 5 is the result of work on a variety of medium carbon steels including 1040, 1330, 4140, 4340, 8630 and others of varying alloy content⁽¹⁹⁾. The variation of rotating-bending fatigue strength at 10^7 cycles with ultimate strength is shown in

Fig. 17. These results indicate that composition and heat treatment have little effect on the long life fatigue strength of cast steels of the same tensile strength and that the unnotched fatigue ratio* is approximately 0.40 to 0.45. Note that as tensile strength increases (Brinell hardness) there is a greater deviation from the line for a fatigue ratio of 0.50. Vishnevsky and Wallace⁽³²⁾ in a similar study of cast 8630 (Ni-Cr-Mo) report fatigue ratios for quenched and tempered as well as normalized and tempered, unnotched, rotating-bending specimens as low as 0.37. In a later study Breznak, et al.⁽³³⁾ cite an endurance ratio for plate bending of 0.13 for a quenched and tempered ($S_u = 138$ ksi) 8630 cast steel with Class 6** shrinkage and 0.17 for a similar strength steel but with Class 2 shrinkage.

Table 6 shows a summary of their results. Steels No. 10 and 11 are radiographically "sound" and No. 10 has a higher strength than No. 11. However, the "endurance" ratio of No. 10 is 0.28 compared to 0.35 for the lower strength steel. Even though considered radiographically "sound," the composition of steel No. 10*** is within the region that Turkdogan and Grange⁽⁹⁾ designate as "blowholes" (Fig. 7). Secondly, the ductility of No. 10 was reported as 25.5% RA, which is consistent with Sims and Dahles⁽⁵⁾ contention that Type II sulfide inclusions are possibly present.

Other interesting aspects shown in Table 6 are (i) that for equivalent composition and strength, the materials with the greatest severity of shrinkage have lower "endurance" limits and ratios, (ii) materials with lower strengths (hardness) are less prone to the degradation in fatigue resistance caused by internal defects, (iii) the greater the strength (hardness), the lower the "endurance" limits and ratios

$$\text{*Fatigue ratio or "endurance" ratio} \equiv \frac{\text{Fatigue strength at } 10^7 \text{ cycles}}{\text{Ultimate tensile strength}}$$

**ASTM E-71

***0.35 w/o C; 0.21 w/o Mn; 0.15 w/o Si; 0.69 w/o Cr; 0.74 w/o Ni; 0.40 w/o Mo; 0.016 w/o P; 0.017 w/o S; 0.19 w/o Al.

(shrink class the same), (iv) shrinkage cavities extending to the surface of a bending specimen show a more pronounced decrease on the "endurance" limit and ratios. The last observation is an agreement with Turnbull, et al.⁽³⁴⁾ who conclude that shrinkage porosities at or near the center of plate or bar steel castings have no significant influence on bending fatigue strength and even severe, Class 2, shrinkage at the surface results in a loss of only 20% compared to radiographically "sound" samples. Unfortunately the hardness of the 8630 cast steels used in these experiments was approximately 200 BHN and a significant decrease in fatigue strength should not have been expected.

Many of the previously cited investigators^(19, 32, 33, 34) have included as part of their programs, a study of the effect of geometric notches on the fatigue behavior of cast steels of various compositions and heat treatments. Table 5 and Fig. 17 show the results of Evans, et al.⁽¹⁹⁾ in which both the notched wrought and notched cast steel data lie within the same banded region on the endurance limit versus tensile strength plot. Results shown in Tables 7 and 8 for notched cast steels^(32, 35) also fall within this band. Conclusions drawn by the authors are (1) that the presence of geometric notches reduce the endurance limit of both wrought and cast steels, (2) this effect is greater the higher the tensile strength (hardness) and (3) notches affect cast steels less than wrought steels (i. e. cast steels are less notch sensitive)⁽³⁶⁾.

Conclusions (1) and (2) are well documented by Peterson for geometric notches in wrought steels. Also, Fig. 18⁽³⁷⁾, which appears in an excellent review by La Pointe⁽³⁸⁾ on the role of inclusions on the fatigue behavior of steels, shows that inclusions* affect the fatigue resistance of even a moderate strength (125 ksi UTS) steel. Since cast steels also contain microdiscontinuities, they are also "metallurgically"

*Depending on shape and size according to their Fairey Count.

notched. By the common definition of the fatigue notch factor:

$$K_f = \frac{\text{Unnotched fatigue strength}^*}{\text{Notched fatigue strength}}$$

conclusion (3) appears in error, since an a priori assumption that the cast steels are "unnotched" is obviously incorrect. A more representative fatigue notch factor could be obtained by using fatigue data obtained from testing wrought steel of comparable hardness, composition and structure to the matrix of the cast metal⁽³⁹⁾ and using this value as "unnotched fatigue strength."

Surface Finish

Burdon⁽³¹⁾ points out that differences in fatigue strength due to differently heat treated cast steels may be small when compared to variations it is possible to obtain from varying the quality of the surface finish. Figure 19 demonstrates the percent reduction in fatigue strength due to various surface finishes ranging from fine polish, as the basis, to unmachined. As shown, with increasing strength (hardness) of the castings, a proportionate decrease occurs in fatigue strength ranging to as great as 70% reduction for a UTS of 200 ksi (approx. 400 BHN). Evans, et al.⁽¹⁹⁾ report the endurance limit is the same for cast steels with polished and lathe turned surfaces, whereas for wrought steels the endurance limit is 22% lower for the lathe turned surface. For comparable lathe turned surfaces, the endurance limit of both wrought and cast steels is approximately equal.** Unfortunately surface residual stress measurements were not included in either of the preceding reports for as Sinclair, et al.⁽⁴⁰⁾ demonstrate, residual stress influences fatigue strength at long lives to a greater degree than surface roughness.

*At some finite life, say, 10^7 cycles.

**The maximum hardness obtained for cast steels used in these tests was 375 BHN.

Directionality

As mentioned previously, for wrought steels, the endurance limit is appreciably lower in the transverse direction than in the longitudinal direction of prior working. This is attributed to the elongation of inclusions in the direction of prior working and the stress concentrating effect of loading normal to the major axis of an essentially elliptical void. Cast steels, however, do not exhibit this directionality since the microdiscontinuities have no preferential orientation. It is also common practice to liken the fatigue resistance of cast steels to those of a comparable wrought steel tested in a transverse direction^(12, 13, 19).

Size (Mass)

Increasing size or mass of steel castings has already been shown (Fig. 8) to have a deleterious effect on mechanical properties. Since composition and heat treatment were also shown to affect tensile strength and therefore fatigue strength, it is reasonable to assume a similar decrease in fatigue resistance due to increasing mass. Figure 20 demonstrates a trend to lower "endurance" limits in passing from the surface to the center of various cast steel sections⁽¹⁹⁾. If the "endurance" limit were only dependent on tensile strength at various sections of a casting, a plot of "endurance" ratio versus section size would be a horizontal line. Such, however, is not the case as demonstrated by Fig. 21 for the 8635 N & T and Q & T condition. Compared to the lower hardness (approx. 150 BHN) 1030 castings, there is a decrease in endurance ratio with section size increase. It was concluded that grain size, increase in inclusion size and changes in microstructure produced this decrease, however such "contributors" to this decrease were difficult to isolate.

Applied Stress System

Several papers^(32, 33, 35) include fatigue results from reversed torsion and plate bending tests on cast steels. Invariably, theories of elasticity are employed

for an homogeneous isotropic material with the hope of obtaining a constant relationship or ratio between the shear and tensile stresses causing fatigue failures. Table 9 shows a comparison of the various yield criteria of failure for tension and torsion tests⁽⁴¹⁾. Presuming that at long lives there is "elastic" behavior, the predicted value of the fatigue strength in torsion to that in bending is:

$$\begin{aligned} &0.5 \quad (\text{Max. Shear Stress}) \\ \frac{FS_t}{FS_b} &= 0.577 \quad (\text{Max. Strain Energy}) \\ &1.0 \quad (\text{Max. Normal Stress}) \end{aligned}$$

Cast steels are not homogeneous isotropic materials. They are internally defected structures. So, for simplicity, assume a hole in an infinite plate subjected to several modes of loading as shown in Fig. 22⁽⁴²⁾. A maximum two-dimensional theoretical stress concentration factor of $K_t = 3$ exists in uniaxial tension* due to the tensile stress field while $K_t = -1$ at the compressive stress field⁽⁴¹⁾. The same is true for uniaxial compression but the stress fields change position by 90° . For torsion (Fig. 22), an element at 45° to the shear forces will be described by a superposition of the two aforementioned cases. In this instance the maximum value of the theoretical stress concentration factor is, $K_t = 4$ for both the tensile and compressive stress fields.

Fatigue failure will initiate at the location where the stress concentration is maximum. Regardless of the failure criterion used, the maximum stress (σ_1) at the initiation site will be the same because all yield envelopes cross at that point as shown in Fig. 23⁽⁴³⁾. Consequently, the fatigue strength in torsion should be $3/4$ that in bending (Fig. 24) presuming other factors constant, that is:

$$\frac{FS_t}{FS_b} = \frac{3}{4} \quad (\text{with circular stress concentration})$$

*The stress state at the outer fibers of a plate in bending.

Figure 25⁽³⁵⁾ shows a plot of "endurance" ratio in torsion (t) to that in bending (b) for notched, wrought steels. Data points shown are from Ref. 44. Dashed lines represent the distortional energy theory and maximum shear stress theory lines for $t/b = 0.577$ and 0.5 , respectively. The data points for the "drilled hole" show best agreement to $t/b = 3/4$ developed in the previous argument. Vee-notch specimens (55° circumferential) deviate slightly, due to a difference in stress concentration, but are still in better agreement with $t/b = 3/4$. In fact, from similar arguments for elliptical holes in orientations producing the largest value of K_t in torsion defined as

$$K_t = 2 \left[\frac{b}{a} + 1 \right]$$

where;

b = major axis of ellipse

a = minor axis of ellipse

compared to bending will result in the limiting case as $t/b = 1$.

Cast metals have t/b ratios which vary between 0.7 to 1.05 ⁽³⁵⁾ (avg. = 0.85) and, as such, would also be in better agreement with the above concept (i.e., they are "internally notched" to begin with). However, in an analysis of their results shown in Table 10, Vishnevsky, et al.⁽³⁵⁾, conclude that "all the points except one lie above the Maxwell-von Mises criterion indicating that discontinuities present in torsion are not nearly so damaging as they are in bending." It is obvious from Table 10 that the endurance ratios in torsion are lower than those in bending and that the t/b ratio averages of 0.85 and 0.79 for the Q & T and N & T condition are also in agreement with the present argument.

Defects

Fatigue resistance of cast steels is dependent on the nature of internal micro-discontinuities as can be surmised from the previous sections of this report. Particular attention to the works of de Kazinczy⁽⁴⁵⁻⁵¹⁾, who has published prolifically

on this topic, will be made in this section. It will be demonstrated that the size, shape and location of defects as well as the strength (matrix hardness) of the cast steels governs fatigue resistance. A proposed course for future research, with particular emphasis on a local stress-strain analysis, will also be presented.

From the work of Evans, et al.⁽¹⁹⁾ on the effect of section size, it was postulated that the lower "endurance" ratio for specimens from the center of large castings compared to specimens from the surface was due to microshrinkage cavities, voids, etc. This was a reasonable assertion since, as has been demonstrated, increasing section sizes lead to decreased solidification rates which, in turn, result in larger defect sizes. In earlier work, de Kazinczy⁽⁴⁵⁾ investigated defects at the origin of fatigue cracks of several medium carbon cast steels in order to evaluate their effect on fatigue strength. To characterize the defects, two parameters were used: (1) defect size - the diameter of the smallest circle enclosing the defect originating failure as it appeared on the fracture surface, and (2) the smallest distance between the defect and the specimen surface. Fracture initiating defects were subdivided into four ranges (1) < 0.02 in., (2) 0.02 to 0.06 in., (3) 0.06 to 0.12 in., (4) > 0.12 in. Table 11 shows the results of these tests conducted with the probit test method⁽⁵²⁾. Microshrinkage cavities extending to 0.004-0.008 in. below the specimen surface were the origin of failure in 77% of the tests, slag layers and sulfide inclusions accounted for 17% while fractures due to spherical inclusions accounted for the remainder. Excluding spherical defects, the endurance limit (σ_e) at 2×10^7 cycles for these tests as a function of defect size (d in inches) was determined to be

$$\sigma_e = 28.5 (1 + 0.8 d^{\frac{1}{2}})^{-1} \text{ ksi}$$

for an UTS range of 58-75 ksi.

From the preceding equation, a value of 28.5 ksi would be a "defect free endurance limit." Rearranging terms and defining the fatigue notch factor;

$$K_f = \frac{\text{"defect free endurance limit"}}{\text{"defect endurance limit"}} = \frac{\sigma_o}{\sigma_e}$$

$$\therefore K_f = (1 + 0.8 d^{\frac{1}{2}})$$

From a maximum defect size of $d = 0.35$ inches; $K_f \approx 1.5$.

Results from work on nodular iron⁽⁵³⁾ with tensile strengths of approximately 70-135 ksi in which microcavities from 0.002-0.01 inches in diameter initiated fatigue failures, showed fatigue notch factors of from 1.4 to 2.0. Weld fissures with a diameter of 0.11 inches in a Ni-Cr-Fe alloy with an ultimate strength of approximately 86 ksi caused a fatigue notch factor of $K_f = 2.3$ ⁽⁵⁴⁾. De Kazinczy's value of K_f , does not account for variations in the shape of defects or matrix strength (hardness) which have been shown^(20, 22, 24, 36, 37, 39, 53-62) to influence fatigue resistance of ferrous-based metals. Granted, the matrix hardness of the cast steel in de Kazinczy's work is low (approximately 120-150 BHN) and fatigue notch factors would be correspondingly low, however, it is inadvisable to employ his results to higher hardnesses or ferrous-based castings with different defect morphologies.

In an attempt to employ the equation of the form:

$$\sigma_e = \sigma_o (1 + a d^{\frac{1}{2}})^{-1}$$

where; σ_e = "endurance limit" of cast steel

σ_o = "defect free endurance limit"

a = constant

d = diameter of smallest circle enclosing defect initiating failure

de Kazinczy⁽⁴⁹⁾ partially accounts for defect geometry by introducing a second constant. The equation is modified to the form:

$$\sigma_e = \sigma_o \left[1 + \left(\frac{\sigma_y d^{\frac{1}{2}}}{K} \right)^{-1} \right]$$

where; K = a constant representing defect geometry

σ_y = yield strength

Thus, "a" from the previous equation is the quotient of σ_y to K . By plotting alternating stress from probit tests results versus defect size, as typified by Fig. 26, the "defect free" value of σ_o is obtained. Solution of simultaneous equations result in the notch effect parameter "a." Figure 27 shows the notch effect parameter versus yield strength of the cast metals from several of de Kazinczy's papers as well as points for a Ti-6 Al-4V alloy⁽⁶³⁾.

Noting that the fatigue strength of wrought steels is often related to tensile strength, de Kazinczy introduces a third equation:

$$0.5 \sigma_m - \sigma_e = B d^{1/5}$$

where; σ_m = ultimate tensile strength

B = a constant

Table 12 lists all constants in the above equations for tensile strengths from 65-150 ksi, varying specimen diameters, various load modes, defect types and locations, etc. Finally, a plot is made of endurance limit versus tensile strength as a function of defect size (Fig. 28) and it is noted that the endurance limit reaches a maximum depending on defect size and ultimate strength (hardness). Figure 28 is quite similar to Fig. 29 in which Garwood, et al.⁽⁶⁴⁾ show a similar maximum in endurance limit versus hardness for wrought steels. Note the maximum endurance limit is dependent on carbon content (maximum obtainable as-quenched hardness) and the Rockwell hardness at which the maximum endurance limit occurs increases with carbon content.

Assuming the inclusion size in the wrought steels to be constant, the maximum obtainable endurance limit appears to be a function of the amount of retained austenite. Table 13 shows the maximum as-quenched hardness (dependent on carbon content)⁽⁶⁵⁾, the peak hardness at which the endurance limit occurred (Fig. 29) and the volume percent retained austenite⁽⁶⁶⁾. Figure 30 shows the relation of hardness and retained austenite as a function of carbon content. It is possible for the retained austenite to preferentially surround inclusions high in carbon (carbides) and upon straining transform to martensite. This would cause a self-induced compressive stress to be produced on the inclusions due to the volume transformation of $\gamma \rightarrow$ martensite⁽⁶⁷⁾. As such, there would be a proportional increase in the maximum obtainable endurance limit depending on the amount of retained austenite.

Although the peak endurance limit for the cast steels is more strongly dependent on size of discontinuity, it is possible to take advantage of metallurgical transformations and improve fatigue performance. Cooling the castings rapidly results in a decrease in the size of microcavities. Sulfide inclusions, however, will still be present. As Turkdogan and Grange⁽⁹⁾ demonstrate, the sulfide inclusions act as nuclei for the precipitation for the ferrite phase during decomposition of austenite. By surrounding the sulfides in a "softer," more compliant material, the local fatigue notch factor can be reduced thus improving the materials fatigue resistance.

Ouchida, et al.⁽⁶²⁾ further investigated the effect of defect size on the fatigue strength of carbon-steel castings with ultimate strengths of 65.6-74.7 ksi. As with Briggs, et al.⁽³⁵⁾, one of the main conclusions in their research was that the fatigue strength of specimens having drilled holes was approximately equal to cast specimens having blowholes of the same (maximum) size. De Kazinczy⁽⁴⁷⁾ substantiates that the largest defects are of major importance. His research on the effect of 2000°A thick NbC precipitates showed that microshrinkage cavities were the initiation sites for fatigue fracture in every sample tested.

Conclusions and Recommendations

From the foregoing review, it appears that the fatigue resistance of cast steels is dependent on (1) size, (2) shape, (3) distribution of microdiscontinuities as well as (4) the strength (hardness) and ductility of the matrix. In order to adequately predict the fatigue resistance of cast metals, all these factors must be taken in account.

Much of our present understanding of the fatigue behavior of metals has been gathered using smooth laboratory samples of wrought products. Experimental results are generally obtained by testing wrought metals at constant strain or stress amplitudes until failure. Further the effect of geometric notches and their influence on fatigue performance of metals is obtained by additional testing of notched members of the same wrought metal and comparing the attainable "notched" and "unnotched" stress or strain levels at a finite life.

In lieu of exhaustive and expensive testing, predictive techniques are employed to quantitatively ascertain the "size" of the geometric notches. One of the more popular is attributed to Peterson⁽³⁶⁾ and is expressed as:

$$K_f = 1 + \frac{K_t - 1}{1 + a/r}$$

where: K_f = fatigue notch factor due to a geometric notch.

Peterson's expression employs the theoretical stress concentration factor, (K_t) the tip radius of the geometric discontinuity (r) and a material constant (a) which for most ferrous-based metals can be approximated in inches by⁽⁶⁸⁾

$$a = \left[\frac{S_{ult.}}{300 \text{ ksi}} \right]^{-1.8} \times 10^{-3}$$

If fatigue results for unnotched and notched samples are available, it is often convenient to calculate the material constant (a) knowing the values of r and K_t .

From this, the fatigue notch factor for other size notches and other values of K_t may be determined.

To account for plasticity effects at the "tip" of the discontinuity, Neuber⁽⁶⁹⁾ proposed that theoretical stress concentration factor for a notch in a two-dimensional state of shear stress was equal to the geometric mean of the stress (K_σ) and strain (K_ϵ) concentration factors:

$$K_t = \sqrt{K_\sigma K_\epsilon}$$

Topper, et al.⁽⁷⁰⁾ extended Neuber's analysis fatigue to loading of notched specimens by replacing K_t with K_f and inserting the expressions for K_σ and K_ϵ as

$$K_f = \left(\frac{\Delta\sigma}{\Delta S} \frac{\Delta\epsilon}{\Delta e} \right)^{\frac{1}{2}}$$

where: $\Delta\sigma$ and $\Delta\epsilon$ = local maximum stress and strain ranges at the notch root

ΔS and Δe = nominal stress and strain ranges applied to a notch member

Topper's relation permits life data for notched and unnotched specimens to be plotted as a master curve. With such a master curve, testing a single notch geometry will allow estimates of the fatigue life for other notch configurations in the same material.

Mitchell⁽³⁹⁾ further extended Topper's analysis to cast metals which have inherent microdiscontinuities or metallurgical defects. He treated the graphite flakes in gray cast iron as "internal notches." By fatigue testing both gray cast irons and wrought steels matched in hardness, structure and composition to the matrix of several different gray irons, he quantitatively assessed the fatigue notch factor for various graphite morphologies and matrix hardnesses. A master plot employing the aforementioned Neuber-Topper relationship was thereby produced.

Proposal

From the preceding discussion it is deduced that a quantitative prediction of the fatigue performance of cast metals requires extensive testing of comparable cast and wrought metals. On the other hand, an a priori metallographic examination of the cast metal can be done to statistically describe the microdiscontinuities.

Using techniques similar to those developed by Schwartz and Saltykov⁽¹¹⁾, it appears possible to extrapolate distribution curves for microdiscontinuities in cast metals to ascertain the "largest." Approximating "flake-shaped" flaws as a pattern of ellipses, spherical flaws as a pattern of spheres, etc., as shown in Fig. 31⁽⁷¹⁾, a value of K_t can be obtained. A form of the equation for the material constant (a) can be modified to:

$$a = \left[\frac{0.5 \text{ BHN}}{300 \text{ ksi}} \right]^{-1.8} \times 10^{-3} \text{ inches}$$

where the ultimate strength, which is "flaw" sensitive, is replaced by one-half the matrix hardness.* Using the appropriate value of "tip" radius, r , K_f can be determined by

$$K_f = 1 + \frac{K_t - 1}{1 + a/r}$$

Once this is accomplished, a Neuber-Topper master curve for the matrix steel, an example of which is shown in Fig. 32, can be determined from a predicted strain-life curve⁽⁶⁸⁾ by the geometric mean of the product of the stress range, strain range and modulus of elasticity at given life levels. Using the modified equation:

$$K_f (\Delta S \Delta \epsilon E_c)^{\frac{1}{2}} = (\Delta \sigma \Delta \epsilon E_s)^{\frac{1}{2}}$$

*The insertion of BHN in the equation does not imply that one should actually perform a Brinell measurement. Matrix microhardness measured with a Vickers, Knoop or other superficial indentors should be converted to an equivalent Brinell number.

where E_c = modulus of elasticity of cast metal
 E_s = modulus of elasticity of wrought metal*

and inserting the value of K_f previously determined, a means of predicting the fatigue resistance for the cast metal is accomplished.

*These are substituted because in the assumption of nominally elastic response, $\Delta S = \Delta \epsilon E_c$, the equation reduces to $K_f \Delta S = [\Delta \sigma \Delta \epsilon E_s]^2$

REFERENCES

1. Sims, C. E., "The Nonmetallic Constituents of Steel," the 1959 Howe Memorial Lecture, AIME Trans., Vol. 215, June, 1959, pp. 367-393.
2. Hilty, D. C. and Crafts, W., "Solubility of Oxygen in Liquid Iron Containing Silicon and Manganese, AIME Trans., Vol. 188, 1950, pp. 414-424.
3. Sims, C. E. and Lillieqvist, G. A., "Inclusions - Their Effect, Solubility and Control in Cast Steel," AIME Trans., Vol. 100, 1932, pp. 154-193.
4. Flemings, M. C., "The Solidification of Castings," Scientific American, Vol. 231, No. 6, Dec., 1974, pp. 88-95.
5. Sims, C. E. and Dahle, F. B., "Effect of Aluminum on the Properties of Medium Carbon Cast Steel," AFA Trans., Vol. 46, 1938, pp. 65-132.
6. Sims, C. E. and Dahle, F. B., "Comparative Quality of Converter Cast Steel," ASTM Proc., Vol. 42, 1942, pp. 532-550.
7. Young, E. R., "Making Steel Castings to Specification," AFA Trans., Vol. 29, 1921, p. 245.
8. Urban, S. F. and Chipman, J., "Nonmetallic Inclusions in Steel, Part II Sulphides," ASM Trans., 1935, pp. 645-671.
9. Turkdogan, E. T. and Grange, R. A., "Microsegregation in Steel," JISI, Vol. 208, Part 5, May, 1970, pp. 482-494.
10. Turkdogan, E. T., "Deoxidation of Steel - What Happens From Tap to Solidification," J. Metals, AIME, 1967, Vol. 19, pp. 38-44.
11. Underwood, E. E., Quantitative Stereology, Addison-Wesley Publishing Company, Reading, Massachusetts, 1970.
12. ASM Metals Handbook, Vol. 1, 8th Edition, "Steel Castings," pp. 122-146 and 206-209, American Society Metals, Metals Park, Ohio, 1961.
13. McNaughton, J. D., "Carbon and Low Alloy Steels," Machine Design, 1970 Metals Reference Issue, Vol. 42, February 12, 1970, pp. 13-17.
14. "Summary of Steel Castings Specifications," Specifications Committee, Steel Founders' Society of America, Rocky River, Ohio, 1971.
15. The Making, Shaping and Treating of Steel, "Castings - Steel and Iron-Section 1," Chapter 38, United States Steel Corp., Edited by H. E. McGannon, 8th Edition, 1964, pp. 1006-1026.
16. Sinclair, G. M. and Dolan, T. J., "Some Effects of Austenitic Grain Size and Metallurgical Structure on the Mechanical Properties of Steel," ASTM Proc., Vol. 50, 1950, pp. 587-618.

17. Landgraf, R.W., Mitchell, M.R. and LaPointe, N.R., "Monotonic and Cyclic Properties of Engineering Materials," Ford Motor Company, Scientific Research Staff Special Technical Publication, June, 1972.
18. Grover, H.J., Gordon, S.A. and Jackson, L.R., "Fatigue of Metals and Structures," NAVAER 00-25-534, Bureau of Aeronautics, Dept. of the Navy, 1954.
19. Evans, E.B., Ebert, L.J. and Briggs, C.W., "Fatigue Properties of Cast and Comparable Wrought Steels," ASTM Proc., Vol. 56, 1956, pp. 1-32.
20. Landgraf, R.W., "Cyclic Deformation and Fatigue Behavior of Hardened Steels," T. &A.M. Report No. 320, Theoretical and Applied Mechanics Department, University of Illinois, Urbana, Illinois, November, 1968.
21. McKenzie, J.T., "The Brinell Hardness of Gray Irons and Its Relation to Some Other Properties," ASTM Trans., Vol. 46, 1946, pp. 1025-36.
22. Testin, R.A., "A Review of the Mechanical Properties of Nodular Cast Iron with Special Reference to Fatigue," Fracture Control Program Report No. 2, College of Engineering, University of Illinois, Urbana, Illinois, March, 1972.
23. Wyman, L.L. and Moore, G.A., "Quantitative Metallographic Evaluations of Graphitic Microstructures," Modern Castings, Vol. 43, No. 1, January, 1963, pp. 7-16.
24. Shul'te, Yu. A., Volchok, I.P. and Pinchuk, E.I., "Nonmetallic Inclusions and the Failure of Cast Steels," Russian Casting Production, No. 3, March, 1971, pp. 114-115.
25. Kotsyubinskii, O., Yu. and Oberman, Ya., I., "Influence of Graphite Particles on the Plastic Deformation and Warping of Iron Castings," Russian Castings Production, Vol. 4, 1967, pp. 185-191.
26. Lorig, C.H. and Elsea, A.R., "Occurrence of Intergranular Fracture in Cast Steels," AFA Trans., Vol. 55, 1947, pp. 160-174.
27. Woodfine, B.C. and Quarrell, A.G., "Effect of Al and N on the Occurrence of Intergranular Fracture in Steel Castings," JISI, Vol. 195, Part 4, August, 1960, pp. 409-414.
28. Wright, J.A. and Quarrell, A.G., "Effect of Chemical Composition on the Occurrence of Intergranular Fracture in Plain Carbon Steel Castings Containing Aluminum and Nitrogen," JISI, Vol. 200, Part 4, April, 1962, pp. 299-307.
29. Altmann, P., Van Eeghem, J.R. and Vinckier, A.G., "Rock Candy Fracture in a Cast Steel," Applied Materials Research, Vol. 4, January, 1965, pp. 20-24.
30. Steel Casting Design, Engineering Data File, Section 5, "General Properties," Steel Founders' Society of America, Rocky River, Ohio, 1968.

31. Burdon, E.S., "The Requirements for Fatigue Strength Data on Steel Castings," S.C.R.A.T.A. Proceedings of 1968 Annual Conference, Paper 3, pp. 1-10.
32. Vishnevsky, C. and Wallace, J.F., "Fatigue of Cast Steels, Part I-A Study of the Notch Effect and of Specimen Design and Loading on the Fatigue Properties of Cast Steel," AFS Cast Metals Res. Jol., Vol. 4 No. 2, June, 1968, pp. 95-101.
33. Breznak, E.S., Vishnevsky, C. and Wallace, J.F., "The Effect of Internal Shrinkage Discontinuities on the Fatigue and Impact Properties of Cast Steel Sections," Steel Foundry Research Foundation, Rocky River, Ohio, May, 1969.
34. Turnbull, G.L., Wallace, J.F. and Briggs, C.W., "Effect of Shrinkage Porosity on Mechanical Properties of Steel Casting Sections," ASM Trans., Vol. 55, 1962, pp. 319-334.
35. Vishnevsky, C., Bertolino, N.F. and Wallace, J.F., "The Effects of Surface Discontinuities on the Fatigue Properties of Cast Steel Sections," Steel Foundry Research Foundation, Rocky River, Ohio, August, 1966. Also same title published by Briggs, C.W., Wallace, J.F., Vishnevsky, C. and Bertolino, N.F., as ASME No. 67-WA/MET-17, August, 1967.
36. Peterson, R.E., "Notch-Sensitivity," Chapter 13, Metal Fatigue, edited by G. Sines and J.L. Waisman, Univ. of Calif. Engineering Extension Series, McGraw-Hill, 1959, pp. 293-306.
37. Atkinson, M., "The Influence of Non-metallic Inclusions on the Fatigue Properties of Ultra-High Tensile Steels," JISI, May, 1960, pp. 64-74.
38. LaPointe, N.A., "The Role of Inclusions in the Fatigue of Steels- A Critical Review," Ford Motor Company, Scientific Research Staff, Metallurgy Dept., Technical Memorandum No. 71-03, January 26, 1971.
39. Mitchell, M.R., "Effects of Graphite Morphology, Matrix Hardness, and Structure on the Fatigue Resistance of Gray Cast Iron," SAE Report No. 750198, February 24, 1975.
40. Sinclair, G.M., Corten, H.T. and Dolan, T.J., "Effect of Surface Finish on the Fatigue Strength of Titanium Alloys RC 130B and Ti 140A," ASME Trans., Jol. of Basic Engineering, Paper No. 55-A-197, 1955.
41. Seely, F.B. and Smith, J.O., Advanced Mechanics of Materials, Second Edition, Twelfth Printing, Wiley and Sons, Inc., New York, August, 1967.
42. Morrow, JoDean, "Failure of Flawed Media," unpublished technical memorandum, Department of Theoretical and Applied Mechanics, University of Illinois, Urbana, Illinois, February, 1970.
43. Mendelson, A., Plasticity: Theory and Application, Macmillan Company, New York, 1968.
44. Thurston, R.C.A. and Field, J.E., "The Fatigue Strength under Bending, Torsional and Combined Stresses of Steel Test Pieces with Stress Concentrations," Proc. Inst. Mech. Engrg., Vol. 168, 1934, pp. 785-796.

45. de Kazinczy, F., "Influence of Metallurgical Defect Size on the Fatigue Properties of Cast Steel," *Jernkont. Ann.*, Vol. 150, No. 7, 1966, pp. 493-506.
46. de Kazinczy, F., "Size Effect in Fatigue of Cast Steels," *JISI*, Jan., 1969, pp. 40-43.
47. de Kazinczy, F., "Effect on Grain-Boundary Precipitates on the Endurance Limit of Cast Steel," *JISI*, Nov., 1969, pp. 1454-1456.
48. de Kazinczy, F., "Fatigue Properties of a Marine Diesel Engine Crank Throw Forging," *European Shipbuilding - Journal of the Ship Technical Society*, Vol. 19, No. 1, 1970, pp. 9-12.
49. de Kazinczy, F., "Effect of Small Defects on the Fatigue Properties of Medium-Strength Cast Steels," *JISI*, Sept., 1970, pp. 851-855.
50. de Kazinczy, F., "Fatigue Strength across Healed Hot Tears in Castings," *JISI*, April, 1971, pp. 310-312.
51. de Kazinczy, F., "Kommer det att Lalla? - Svetslagnings inverkan pa utmattningshallfastheten," *Särtryck ur Svetsen*, No. 5, Sept., 1971, pp. 3-7.
52. A Guide for Fatigue Testing and the Statistical Analysis of Fatigue Data, ASTM, S1P 9I-A, Second Edition, American Society for Testing and Materials, 1963.
53. Testin, R.A., "Characterization of the Cyclic Deformation and Fracture Behavior of Nodular Cast Iron," Dept. of Theoretical and Applied Mechanics, T. & A. M. Report No. 371, Univ. of Illinois, Urbana, Illinois, June, 1973.
54. Yeniscavich, W., "The Effect of Fissures on the Fatigue Strength of Ni-Cr-Fe-Alloys," *Welding Journal*, Welding Research Supplement, Vol. 45, March, 1966, pp. 111-S -123-S.
55. Neuber, H., Kerbspannungslehre, Springer, Berlin, 1937.
56. Kuhn, P., "Influence des Dimensions sur la Fatigue des Pieces Entaillies," *Rev. de Met.*, Vol. 55, No. 9, Sept., 1958, pp. 860-864.
57. Stewart, W.C. and Williams, W.L., "Effects of Inclusions on the Endurance Properties of Steels," *J. Am. Soc. Nav. Eng.*, Vol. 60, 1948, pp. 475-504.
58. Stulen, F.B., Cummings, H.N. and Schulte, W.C., "Relation of Inclusions to the Fatigue Properties of High-Strength Steel," *Proceedings, International Conference on Fatigue of Metals*, London, 1956, pp. 439-444.
59. Cummings, H.N., Stulen, F.B. and Schulte, W.C., "Fatigue Strength Reduction Factors for Inclusions in High-Strength Steels," *Wright Air Development Center, WADC, TR 57-589*, April, 1958.
60. Cummings, H.N., Stulen, F.B. and Schulte, W.C., "Tentative Fatigue Strength Reduction Factors for Silicate-Type Inclusions in High-Strength Steels," *ASTM Proc.*, Vol. 58, 1958, pp. 505-514.

61. Ikawa, K. and Ohira, G., "Fatigue Properties of Cast Iron in Relation to Graphite Structure," AFS Cast Metals Res. Jo., Vol. 3, No. 1, March, 1967, pp. 11-21.
62. Ouchida, H., Chijiwa, K., Hoshino, J. and Nishioka, K., "Fatigue Strength of Carbon-Steel Castings," Bull. JSME, Vol. 10, 1967, pp. 438-448.
63. Lindh, D. V. and Peshak, G. M., "The Influence of Weld Defects on Performance," Welding Journal, Welding Research Supplement, February, 1969, pp. 45s-50s.
64. Garwood, M. F., Zurburg, H. H. and Erickson, M. A., "Correlation of Laboratory Tests and Service Performance," Interpretation of Tests and Correlation with Service, American Society of Metals (ASM), Cleveland, Ohio, 1951.
65. Crafts, W. and Lamont, J. L., Hardenability and Steel Selection, Pitman Publishing Corp., New York, 1949, p. 88.
66. Roberts, C. S., "Effect of Carbon on the Volume Fractions and Lattice Parameters of Retained Austenite and Martensite," Trans. AIME Vol. 197, 1953.
67. Dittmer, D. F., unpublished research on high carbon martensites, Fracture Control Program, College of Engineering, Univ. of Illinois, Urbana, Illinois, 1975.
68. SAE Fatigue Design Handbook, Vol. 4, Society of Automotive Engineers, New York, 1968.
69. Neuber, H., "Theory of Stress Concentration of Shear-Strained Prismatical Bodies with Arbitrary Nonlinear Stress-Strain Law," Trans. ASME Dec., 1961, pp. 544-550.
70. Topper, T. H., Wetzel, R. M. and Morrow, JoDean, "Neuber's Rule Applied to Fatigue of Notched Specimens," Jol. of Materials, JMLAS, Vol. 4, No. 1, March, 1969, pp. 200-209.
71. Peterson, R. E., Stress Concentration Factors, Wiley and Sons, Inc., New York, 1974.

TABLE 1. General Types of Cast Steels

(Reproduced from Ref. 30 by permission of Steel Founders' Society of America, Rocky River, Ohio)

STRUCTURAL GRADES—CARBON STEELS

Tensile Strength, psi	60,000	65,000	70,000	80,000	85,000	100,000
Indicated Application	Low electric resistivity, desirable magnetic properties, carburizing and case hardening grades, excellent weldability	Excellent weldability, medium strength with good machinability and high ductility		High strength carbon steels with good machinability, toughness and excellent fatigue resistance, readily weldable		Wear resistance, hardness
Current Specifications*	ASTM: A27 U.S. 30 60-30 ASTM: A216 WCA SAE: Automotive Grade 0025 AAR: M201 Grade AU Grade AA Military: MIL-S-15083B Class B A.B.S.: Grade 1 Hull	ASTM: A27 65-35 SAE: Automotive Grade 0030 Federal: QQ-S-681d Class 65-35 Lloyds: Class A ASTM: A352 LCB Military: MIL-S-15083B Class 65-35	ASTM: A27 70-36 70-40 ASTM: A216 WCB WCC AAR: M201-53 Class B Military: MIL-S-15083B Class 70-36 A.B.S. Grade 2 Federal: QQ-S-681d Class 70-36	ASTM A 148 80-40 80-50 SAE: Automotive Grade 080 Federal: QQ-S-681d Class 80-40 Military: MIL-S-15083B Class 80-40 Class 80-50	SAE: Automotive Grade 0050A Federal: QQ-S-681d Class 0050A	SAE: Automotive Grade 0050B Federal: QQ-S-681d Class 0050B
A Typical Specification for the Tensile Grade with Requirements listed below	ASTM: A27 Class 60-30	ASTM: A27 Class 65-35	ASTM: A27 Class 70-36	MIL-S-15083B Class 80-40	SAE: Automotive Grade 0050A	SAE: Automotive Grade 0050B

All values listed below are specification minimum values and apply only to the typical specification listed

Tensile Strength, psi	60,000	65,000	70,000	80,000	85,000	100,000
Yield Point, psi	30,000	35,000	36,000	40,000	45,000	70,000
Elongation in 2", %	24	24	22	17	16	10
Reduction in Area, %	35	35	30	25	24	15
Brinell Hardness No.	—	131 ³	—	163 ³	170 ³	207 ³

Values listed directly below are those normally expected in the production of steel castings for the tensile strength values given in the upper portion of the chart.¹ The values are only for general information and are not to be used as design or specification limit values.

Tensile Strength, psi	63,000	68,000	75,000	82,000	90,000	105,000
Yield Point, psi	35,000	38,000	42,000	48,000	55,000	75,000
Elongation in 2", %	30	28	27	23	20	19
Reduction of Area, %	54	48	45	40	38	41
Brinell Hardness No.	131	131	143	163	179	212
Charpy V-Notched Impact Ft-lbs	70°F 12	35	30	35	26	40
	-40°F 5	12	12	10	10	12
Endurance Limit, psi	Unnotched 30,000	30,000	35,000	37,000	39,000	45,000
	Notched 19,000	19,000	22,000	26,000	28,000	31,000
Modulus of Elasticity	30 million psi	30 million psi	30 million psi	30 million psi	30 million psi	30 million psi
Machinability Speed Index ²	HSS 160	135	135	135	120	80
	Carbide 400	230	230	400	325	310
Type of Heat Treatment	Annealed	Normalized	Normalized	Normalized and Tempered	Normalized and Tempered	Quenched and Tempered

* Summary of Steel Castings Specifications available at Steel Founders' Society of America, Westview Towers - 21010 Center Ridge Road, Rocky River, Ohio 44116

¹ Below 8 percent total alloy content.² There are commercial cast steels available at tensile strength levels greater than 200,000 psi. Properties must be checked with the producers.³ SAE Hardness requirement. (Minimum)

TABLE 1 (Continued)

ENGINEERING GRADES—LOW ALLOY STEELS¹

65,000	70,000	80,000	90,000	105,000	120,000	150,000	175,000	200,000 ²
Excellent weldability, low temperature and high temperature service	Excellent weldability, medium strength with high toughness and good machinability, high temperature service		Certain steels of these classes have excellent high temperature properties and deep hardening properties. High resistance to impact, excellent low temperature properties for certain steels, deep hardening properties, excellent combination of strength and toughness, weldable			Deep hardening, high strength, wear resistance and fatigue resistance	High strength, wear resistance, high hardness, and high fatigue resistance	
ASTM: A352 ICB, IC1, IC2, IC3 ASTM: A217 WC1 Military: MIL S 870B	ASTM: A217 WC4, WC5, WC6, WC9 Military: MIL S 15464B Classes 1, 2 and 3	ASTM: A148 80 40 80 30 ASTM: A487 1N, 3N SAE: Automotive Grade 800 Federal: QQ-S-681d Class 80-50 Military: MIL-S-15083B Class 80-50	ASTM: A148 90 60 ASTM: A217 CJ, C12 ASTM: A487 90-60 SAE: Automotive Grade 900 Federal: QQ-S-681d Class 90-60 AAR: M701-47 Grade C Military: MIL-S-15083B Class 90-60	ASTM: A148 105 85 ASTM: A487 JQ, 4Q, 5Q 8Q, 9Q 5N Federal: QQ-S-681d Class 105-85 Military: MIL-S-15083B Class 105-85 SAE: Automotive Grade 1103	ASTM: A148 120 95 ASTM: A487 6Q SAE: Automotive Grade 1120 Federal: QQ-S-681d Class 120-95 Military: MIL-S-15083B Class 120-95	ASTM: A148 150-125 SAE: Automotive Grade 0150 Federal: QQ-S-681d Class 150-125 Military: MIL-S-15083B Class 150-125	ASTM: A148 175-145 SAE: Automotive Grade 0175 Federal: QQ-S-681d Class 175-145	None specified
ASTM: A352 Class IC1	ASTM: A217 Class WC4	ASTM: A148 Class 80-50	ASTM: A148 Class 90-60	ASTM: A148 Class 105-85	ASTM: A148 Class 120-95	ASTM: A148 Class 150-125	ASTM: A148 Class 175-145	None specified

All values listed below are specification minimum values and apply only to the typical specification listed

65,000	70,000	80,000	90,000	105,000	120,000	150,000	175,000	---
35,000	40,000	50,000	60,000	85,000	95,000	125,000	145,000	---
24	20	22	20	17	14	9	6	---
35	35	35	40	35	30	22	12	---
---	---	163 ³	187 ³	217 ³	248 ³	311 ³	363 ³	---

Values listed directly below are those normally expected in the production of steel castings for the tensile strength values given in the upper portion of the chart.⁴ The values are only for general information and are not to be used as design or specification limit values.

68,000	74,000	86,000	95,000	110,000	128,000	158,000	179,000	205,000
38,000	44,000	54,000	64,000	91,000	112,000	142,000	160,000	170,000
32	28	24	20	21	16	13	11	8
55	50	46	44	48	38	30	25	21
137	143	170	192	217	262	311	352	401
60	55	48	40	58	45	30	24	14
20	22	18	16	40	31	17	12	8
32,000	35,000	39,000	42,000	53,000	62,000	74,000	84,000	88,000
20,000	23,000	25,000	31,000	34,000	37,000	44,000	48,000	50,000
30 million psi	30 million psi	30 million psi	30 million psi	30 million psi	30 million psi	30 million psi	30 million psi	30 million psi
130	120	110	95	90	75	45	35	---
400	230	240	290	310	180	200	180	---
Normalized and Tempered	Normalized and Tempered	Normalized and Tempered	Normalized ⁵ and Tempered	Quenched and Tempered	Quenched and Tempered	Quenched and Tempered	Quenched and Tempered	Quenched and Tempered

⁴ Test values obtained in accordance with ASTM testing procedures. (Relatively large castings show lower ductility values.)

⁵ Machinability speed index for a standard 18-4-1 high-speed steel tool is based on cutting speed which gives one hour tool life. For carbide (788) cutting speed for one hour tool life based on 0.015-inch wearland.

⁶ Quench and temper heat treatments may also be employed for this class.

	Yield Point, ksi	Ultimate Strength, ksi	Elongation Per Cent in 2 In.	% R. A.	Average Izod Impact, Ft-lb
Well dried dry sand mold. No Al used.	47.3 47.8	78.9 79.1	31.5 31.0	54.4 54.9	37.0
Well dried dry sand mold, 0.05 per cent Al added.	50.6 47.9	79.6 79.2	26.5 27.0	38.2 42.0	31.0
Half dried dry sand mold. No Al used.	46.2 47.2	79.5 79.5	31.5 30.5	57.0 54.4	37.0
Half dried dry sand mold, 0.05 per cent Al added.	51.0 51.3	80.3 79.6	26.5 26.5	37.6 38.9	29.0
Air-dried green-sand mold. No Al used.	47.3 45.1	79.3 79.4	32.0 31.5	51.5 56.6	38.5
Air-dried green-sand mold, 0.05 per cent Al added.	49.7 48.9	79.0 79.4	26.0 25.0	36.0 36.6	27.0
Moistened green-sand mold. No Al used.	44.4 47.7	78.8 79.2	31.5 31.5	55.7 56.0	37.0
Moistened green-sand mold, 0.05 per cent Al added.	49.6 50.5	79.3 80.0	24.5 25.0	34.6 35.7	26.5

Composition of steel: C, 0.278 per cent; Mn, 0.79; Si, 0.37; P, 0.030; S, 0.035.
Heat treatment: 1600°F. for 2 hrs. Cooled in still air.

TABLE 2 Mechanical Properties of Test Bars with and without Aluminum⁽³⁾

Heat	Composition				Yield Strength, ksi	Ultimate Strength, ksi	Elong., %	% R. A.	Izod Impact Strength, Ft-lb
	w/o C	w/o Mn	w/o Si	w/o P					
2414	0.27	0.49	0.37	0.018	0.021	44.0	75.0	32.5	55.0
2432	0.24	0.99	0.39	0.019	0.021	52.0	80.0	32.0	56.5
2433	0.26	1.51	0.41	0.017	0.020	60.5	90.0	30.0	62.5
2408	0.28	0.60	0.35	0.018	0.050	44.0	76.5	29.0	48.0
2410	0.25	1.07	0.37	0.022	0.051	57.5	83.0	28.0	47.0
2434	0.27	1.60	0.38	0.019	0.057	64.0	90.0	24.0	36.5
2409	0.29	0.63	0.38	0.019	0.071	48.0	77.5	20.5	22.5
2411	0.26	1.05	0.38	0.021	0.073	56.0	81.5	25.5	34.0
2418	0.26	1.60	0.41	0.020	0.073	65.5	90.0	22.5	27.5

Results shown are average of duplicate tests. All coupons normalized 2 hrs. at 1650°F. followed by a 2 hr. draw at 750°F.

TABLE 3 Effect of Manganese and Sulphur on Mechanical Properties⁽⁵⁾

Heat	Composition						Mechanical Properties				
	w/o C	w/o Mn	w/o Si	w/o P	w/o S	w/o Al Added	Yield Strength, ksi	Ultimate Strength, ksi	Elong., %	R. A.	Izod Impact Strength, Ft-lb
2792	0.28	0.68	3.32	0.016	0.019	---	45.5	75.5	34.0	61.5	51.5
2793	0.28	0.70	3.35	0.015	0.020	0.025	46.5	75.0	32.5	55.5	49.5
2794	0.29	0.69	3.36	0.018	0.019	0.050	46.0	75.0	33.0	58.5	56.5
2795	0.29	0.69	3.38	0.018	0.018	0.10	47.5	76.0	34.0	58.0	64.0
2796	0.31	0.72	3.39	0.018	0.020	0.15	47.0	77.5	31.0	57.5	68.0
3241	0.31	0.79	3.41	0.029	0.019	0.25	55.5	83.5	30.5	54.5	55.0
2797	0.29	0.66	3.27	0.011	0.031	---	44.5	73.5	34.0	56.5	51.0
2798	0.28	0.66	3.27	0.012	0.029	0.025	46.0	73.5	29.5	46.0	40.0
2791	0.29	0.79	3.40	0.012	0.035	0.05	49.5	77.0	31.0	49.0	41.5
2799	0.28	0.65	3.30	0.011	0.031	0.075	45.0	73.0	32.5	53.0	42.5
2800	0.26	0.64	3.28	0.010	0.030	0.10	45.0	71.0	33.0	53.5	52.0
3202	0.28	0.76	3.42	0.017	0.032	0.25	48.0	79.5	30.5	49.0	43.0
2802	0.28	0.62	3.31	0.011	0.041	---	46.5	74.0	32.0	50.5	35.0
2807	0.28	0.67	3.33	0.010	0.044	---	48.5	75.0	33.5	55.0	40.0
2803	0.28	0.65	3.31	0.011	0.037	0.015	46.0	74.5	26.5	35.5	27.5
2808	0.28	0.64	3.32	0.012	0.046	0.015	46.0	74.5	31.5	49.5	37.5
2804	0.29	0.64	3.32	0.012	0.038	0.025	47.0	74.0	26.0	37.0	34.5
2809	0.29	0.68	3.32	0.011	0.045	0.025	47.0	74.0	21.5	25.0	22.5
2805	0.28	0.67	3.32	0.011	0.042	0.05	47.0	74.0	30.0	50.5	36.5
2810	0.28	0.62	3.31	0.011	0.041	0.05	46.0	74.5	30.0	48.0	37.0
2806	0.29	0.63	3.33	0.012	0.040	0.075	48.5	75.0	30.5	47.5	38.5
2811	0.27	0.69	3.35	0.012	0.042	0.075	48.0	74.5	30.0	44.5	34.0
3203	0.28	0.75	3.42	0.020	0.037	0.15	47.0	79.5	31.5	47.5	34.0
3204	0.28	0.80	3.43	0.016	0.039	0.25	51.0	79.5	30.5	48.5	44.0
3205	0.28	0.77	3.38	0.019	0.061	---	46.0	78.5	29.5	46.0	27.0
3206	0.29	0.80	3.42	0.019	0.061	0.015	47.5	77.5	18.5	20.0	18.0
3207	0.29	0.78	3.41	0.019	0.060	0.025	49.0	70.0	26.0	35.5	22.0
3208	0.28	0.72	3.39	0.016	0.062	0.05	46.0	76.5	27.0	38.5	26.5
3209	0.29	0.76	3.42	0.021	0.061	0.10	49.5	78.0	27.0	39.5	29.0
3210	0.28	0.80	3.38	0.016	0.062	0.25	48.5	77.0	28.5	42.0	31.5

All results average of triplicate tests. Heat treatment consisted of normalizing 2 hr. at 1650° F. followed by a draw at 750° F. for 2 hr.

TABLE 4 Effect of Aluminum and Sulphur on Mechanical Properties (5)

Steel	Heat Treatment ^a -F	Tensile Strength, ksi	Yield Strength 0.2 Per Cent Offset, ksi	Reduction of Area, Per Cent	Elongation in 2 in., Per Cent	Brinell Hardness Number	Endurance Limit, ksi		Endurance Ratio	
							Unnotched	Notched	Unnotched	Notched
Annealed ^a										
No. 1	Cast 1040	83.5	49.3	46.7	27.5	156	33.2	26.0	0.40	0.31
No. 2	Wrought 1040	81.4	47.6	54.6	31.0	149	39.3	25.8	0.48	0.32
Normalized and Tempered ^b										
No. 3	Cast 1040	94.2	56.0	52.2	24.5	187	37.7	28.0	0.40	0.30
No. 4	Wrought 1040	90.0	55.7	58.3	26.5	170	43.5	27.2	0.48	0.30
No. 5	Cast 1330	99.3	61.5	58.5	24.0	201	48.4	31.7	0.49	0.32
No. 6	Cast 1330	97.0	63.5	58.5	26.0	201	41.7	31.2	0.43	0.32
No. 7	Wrought 1340	101.3	56.8	60.1	23.5	207	58.7	33.0	0.58	0.32
No. 8	Cast 4135	112.7	86.5	43.1	18.0	223	51.2	33.3	0.45	0.30
No. 9	Wrought 4140	111.1	86.1	62.9	23.4	223	62.0	31.2	0.56	0.28
No. 10	Cast 4335	126.5	100.5	50.2	14.5	262	63.0	34.9	0.50	0.28
No. 11	Wrought 4340	124.6	98.9	63.8	23.5	262	75.5	35.0	0.60	0.28
No. 12	Cast 8630	110.5	85.6	53.7	19.0	223	54.0	33.1	0.49	0.30
No. 13	Wrought 8640	108.5	82.8	60.2	24.0	217	64.5	32.0	0.59	0.30
Quenched and Tempered ^{b, c}										
No. 14	Cast 1330	122.2	106.0	55.6	20.5	269	58.5	37.3	0.48	0.31
No. 15	Wrought 1340	121.2	106.9	60.9	22.5	269	68.4	36.3	0.56	0.30
No. 16	Cast 4135	146.4	131.0	35.8	14.0	311	61.3	40.6	0.42	0.28
No. 17	Wrought 4140	146.8	133.0	60.1	18.5	311	57.4	41.2	0.59	0.28
No. 18	Cast 4335	168.2	155.9	17.8	9.5	375	77.6	48.2	0.46	0.29
No. 19	Wrought 4340	168.4	158.1	56.3	17.0	375	96.5	45.9	0.57	0.27
No. 20	Cast 8630 ^d	137.5	125.8	34.5	14.8	286	64.9	38.6	0.47	0.28
No. 21	Wrought 8640	138.2	124.2	65.6	21.5	286	77.5	37.4	0.55	0.27

^aN = Normalized. T = Tempered. Q = Quenched.

^bAll test specimens were taken from the approximate center of the original material.

^cSlightly oversize test specimens were first machined from the original material in the normalized and tempered condition. These specimens were then water quenched and tempered, and ground-to-size. Tempering was followed by a water quench.

^dTensile test results based on 0.22 in. diam and 0.88 in. gage length.

TABLE 5 Mechanical Properties, Hardness and Fatigue Results of Cast and Wrought Steels⁽¹⁹⁾

Steel No.	Heat Treatment*	Tensile Strength ksi	Endurance Limit ksi	Endurance Ratio	E-71 ASTM Discontinuity
10	Q & T	136.5	38.0	0.28	Sound
11	N & T	83.1	29.0	0.35	Sound
12	Q & T	137.9	23.0	0.17	Shrink Class 2**
12	Q & T	137.9	18.0	0.13	Shrink Class 6**
13	A	91.1	22.0	0.24	Shrink Class 2
13	A	91.1	21.0	0.23	Shrink Class 6
14	Q & T	134.5	36.0	0.27	Shrink Class 2
14	N & T	83.8	27.0	0.32	Shrink Class 2

*Q & T = Quenched & Tempered; N & T = Normalized & Tempered; A = Annealed

**Shrinkage came to the surface of the specimen on machining.

TABLE 6 Plate Bending Fatigue Tests on Samples Containing Shrinkage Discontinuities⁽³³⁾

Heat No.	Heat Treatment*	Tensile Strength ksi	Endurance Limit ksi			Endurance Ratio ^(a)		
			No Notch	Notched in. -R 0.015	Notched in. -R 0.001	No Notch	Notched in. -R 0.015	Notched in. -R 0.001
1	N & T	87.3	34.5	22.0	-	0.395	0.252	-
9	N & T	88.9	-	-	20.0	-	-	0.225
5	N & T	83.4	32.5	20.0	-	0.384	0.240	-
7	N & T	83.1	32.5	21.0	-	<u>0.391</u>	<u>0.253</u>	<u>-</u>
Avg.						0.390	0.248	0.225
6	Q & T	145.0	53.0	32.5		0.366	0.224	-
3	Q & T	126.0	47.0	31.5		0.373	0.250	-
1	Q & T	132.0	-	-	23.0	<u>-</u>	<u>-</u>	<u>0.174</u>
Avg.						0.370	0.237	0.174

*N & T = Normalized & Tempered; Q & T = Quenched & Tempered; R = Radius at bottom of notch in inches; (a)Endurance Limit/Tensile Strength.

TABLE 7 R. R. Moore Fatigue Test Results for 8630 Cast Steels⁽³²⁾

Heat No.	1	9	3	1
Heat Treatment	N & T	N & T	Q & T	Q & T
Tensile Strength (ksi)	87.3	88.9	121.2	132.0
Notch Radius (in.)	0.015	0.001	0.015	0.001
Endurance Limit (ksi)				
Unnotched	34.5	-	47.0	-
Notched	22.0	20.0	31.5	23.0
Endurance Ratio*				
Unnotched	0.395	-	0.390	-
Notched	0.252	0.225	0.255	0.174
K_t^{**}	2.2	6.2	2.2	6.2
K_f^+	1.57	1.73	1.49	2.12
q^{++}	0.475	0.140	0.408	0.216

$$* \text{Endurance Ratio} = \frac{\text{"Endurance Limit"}}{\text{Tensile Strength}}$$

**Theoretical Stress Concentration Factor (K_t)

$^+$ Fatigue Notch Factor

$$(K_f) = \frac{\text{"Endurance Limit" of Unnotched Specimen}}{\text{"Endurance Limit" of Notched Specimen}}$$

$$++ \text{ Notch Sensitivity } (q) = \frac{K_f - 1}{K_t - 1}$$

TABLE 8 R. R. Moore Fatigue Test Results⁽³⁵⁾

Theory of Failure	Maximum Utilizable Strength as Obtained From a Tensile Test	Maximum Utilizable Strength as Obtained From a Torsion Test	Relation between Values of σ_e and τ_e if the Theory of Failure Were Correct for Both States of Stress
Maximum normal stress theory	σ_e	τ_e	$\tau_e = \sigma_e$
Maximum shearing stress theory	$\frac{1}{2} \sigma_e$	τ_e	$\tau_e = 0.50 \sigma_e$
Maximum octahedral stress theory	$\frac{\sqrt{2}}{3} \sigma_e$	$\frac{\sqrt{2}}{\sqrt{3}} \tau_e$	$\tau_e = 0.577 \sigma_e$
Maximum energy of distortion	$\frac{1 + \mu}{3} \frac{\sigma_e^2}{E}$	$(1 + \mu) \frac{\tau_e^2}{E}$	$\tau_e = 0.577 \sigma_e$

TABLE 9 Comparison of Maximum Utilizable Strengths of a Material According to Various Theories of Failure for Each of Two States of Stress, as Occur in the Tension and Torsion Tests⁽⁴¹⁾

Type of Specimen	Endurance Ratio in Bending	Endurance Ratio in Torsion	(t/b)*
Q & T			
Cast Steel-Sound*	0.310	0.298	0.96
Weld-Machine-Sound	0.251	0.230	0.92
Slag Inclusions	0.246	0.246	1.00
As Welded-Sound	0.241	0.221	0.92
Weld-Slag	0.243	0.184	0.75
Weld-Undercut	0.233	0.195	0.84
Cavities	0.117	0.100	0.86
Hot Tears	0.274	0.146	0.53
Avg. = 0.85			
N & T			
Cast Steel-Sound*	0.361	0.270	0.75
Weld-Machine-Sound	0.352	0.261	0.74
As Welded-Sound	0.345	0.250	0.73
Weld-Slag	0.314	0.234	0.75
Weld-Undercut	0.280	0.230	0.82
Cavities	0.235	0.195	0.83
Slag Inclusions	0.292	0.208	0.71
Hot Tears	0.245	0.241	0.98
Avg. = 0.79			

$$*(t/b) = \frac{\text{"Endurance Ratio" in Torsion}}{\text{"Endurance Ratio" in Bending}}$$

***"Endurance Ratio" using R. R. Moore Specimen	Q & T Unnotched	.390
	Q & T Notched (.015" R)	.255
	Q & T Notched (.001" R)	.174
	N & T Unnotched	.395
	N & T Notched (.015" R)	.252
	N & T Notched (.001" R)	.225

TABLE 10 "Endurance Ratios" in Bending and Torsion⁽³⁵⁾

Defect Size (in)	"Endurance Limit" at 2×10^7 Cycles ksi	Standard Deviation ksi
(0.008) - 0.02	25.9	0.92
0.02 - 0.06	24.5	1.49
0.06 - 0.12	22.8	2.4
0.12 - (0.35)	20.6	3.3

TABLE 11 Endurance Limit and Standard Deviation for Different Defect
Size Groups⁽⁴⁵⁾
(UTS Range 58 to 75 ksi)

Tensile Strength, ksi	65.3	71.1	71.1	71.1	71.1	68.2	116.0	127.6	127.6	127.6	150.1	150.1
Yield Stress, ksi	34.8	37.7	39.2	39.2	42.1	50.8	85.6	101.5	101.5	101.5	129.1	129.1
Defect Type*	M (S)	M	P	P	P + M	P	M	M	M	M	M	M
Defect Location [†]	s (i)	s	s	s	i + s	i + s	s	i	s	s	i	s
Specimen diam., in.	0.63	2.56	1.97-3.94	2.76	0.63	0.44	0.44	0.44	0.44	0.44	0.44	0.44
Loading**	TC	R	R	R	TC	TC	TC	TC	TC	TC	TC	TC
σ_o , ksi	27.4	28.8	26.0	28.8	35.8	47.7	51.9	51.9	51.9	51.9	56.2	56.2
a, in. ^{-1/2}	0.81	1.26	2.27	2.02	2.26	2.52	1.21	1.21	3.02	1.86	4.03	4.03
B, in. ^{-1/5} ksi	21.3	22.4	31.3	27.1	-	44.9	40.7	57.1	65.1	84.2	84.2	84.2

*P = pores, blowholes; M = microshrinkage cavities; S = slag inclusions.

[†]i = interior; s = surface.

**TC = tension-compression; R = rotating bending.

TABLE 12 Various Constants for de Kazinczy's Equations⁽⁴⁹⁾

w/o Carbon	R _c (max) [Fig. 30(a)]	R _c (peak) [Fig. 29]	% Retained Austenite [Fig. 30(b)]
0.40	60	45	1
0.50	63	50	2
0.60	65	55	3

TABLE 13 Carbon Content, Maximum As-Quenched Hardness, Peak Hardness at Maximum Fatigue Strength and Percent Retained Austenite in Steel

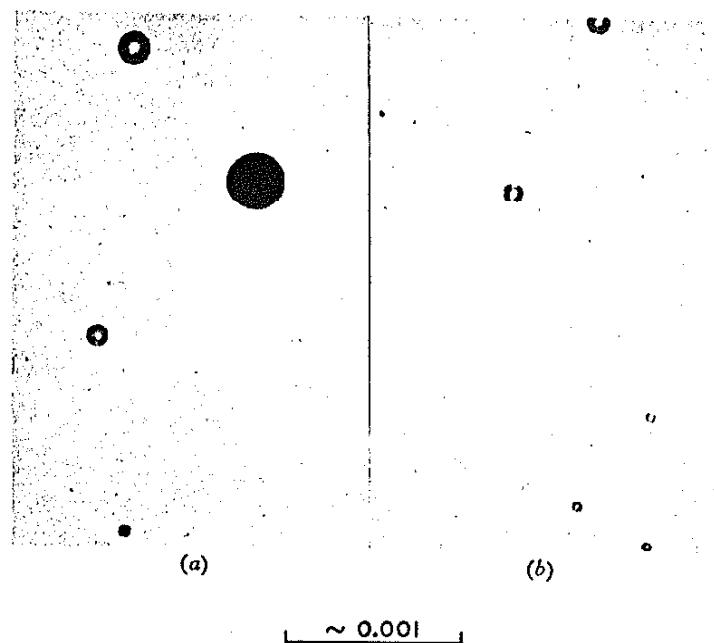


Fig. 1 Effect of Cooling Rate on the Size of Si O_2 Inclusions⁽²⁾

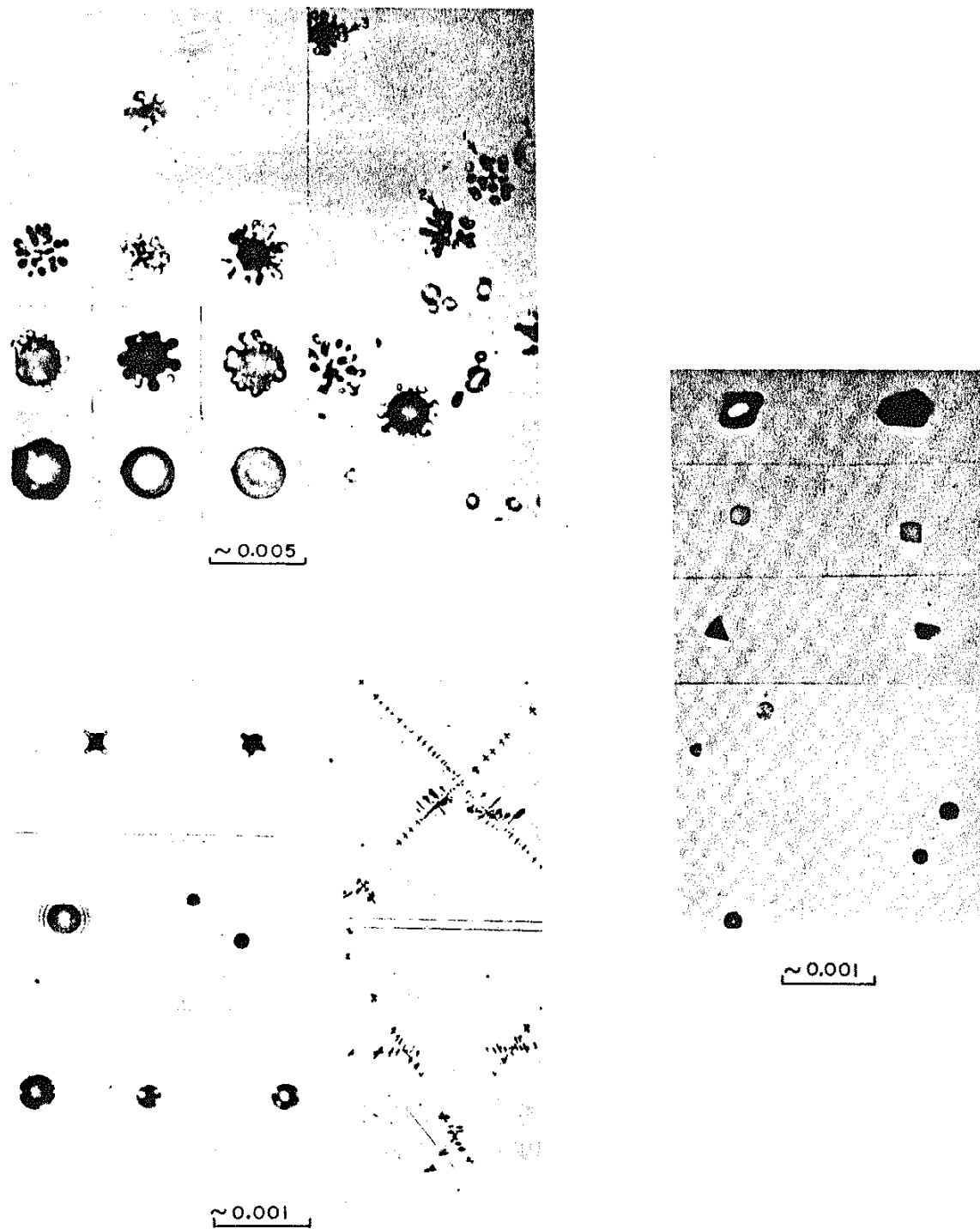
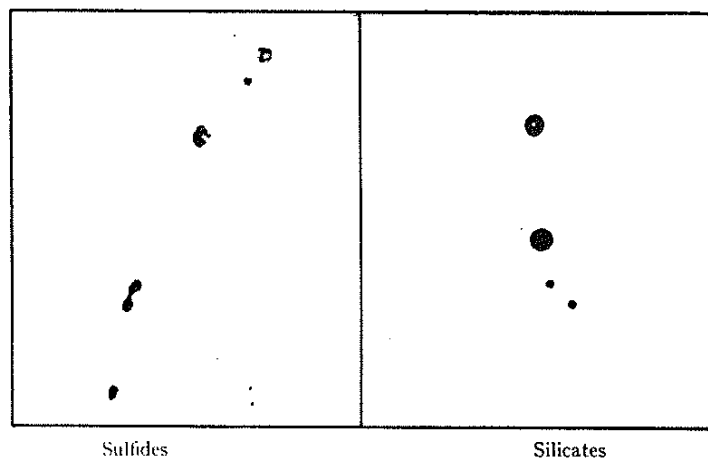
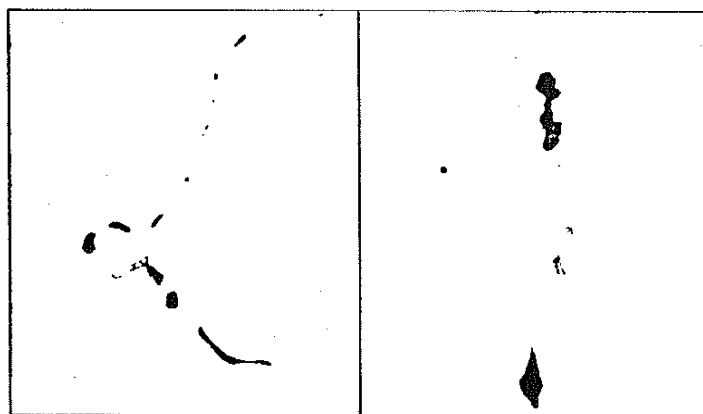


Fig. 2 Several Examples of Variations in Inclusion Shape in Cast Steels⁽¹⁾

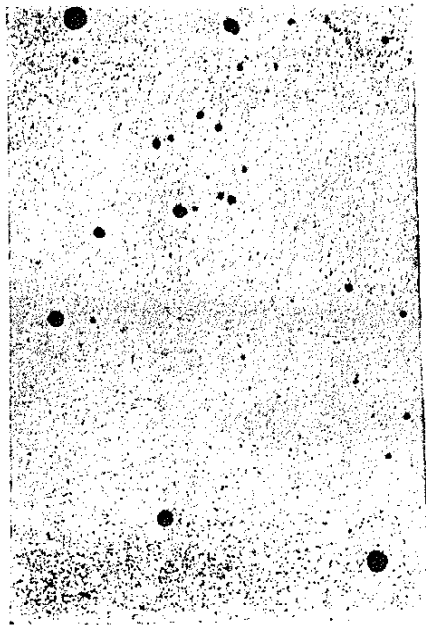


(a) Type I inclusions.

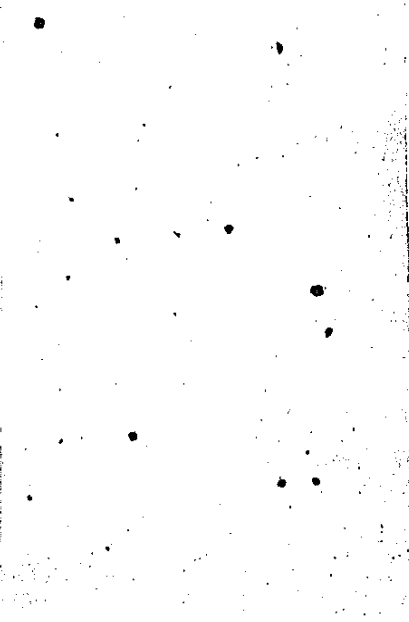


0.005"

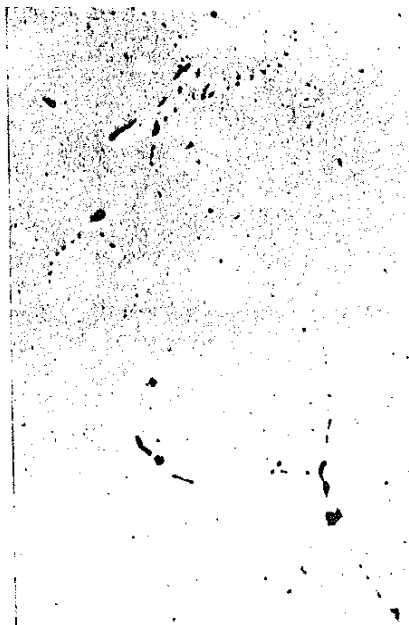
Fig. 3 Type I, II and III Inclusions in Cast Steel⁽⁶⁾



(a)



(b)



(c)



(d)

0.002"

Fig. 4 Effect of Al. Additions on the Shape of Sulfide Inclusions in Cast Steel₁₅

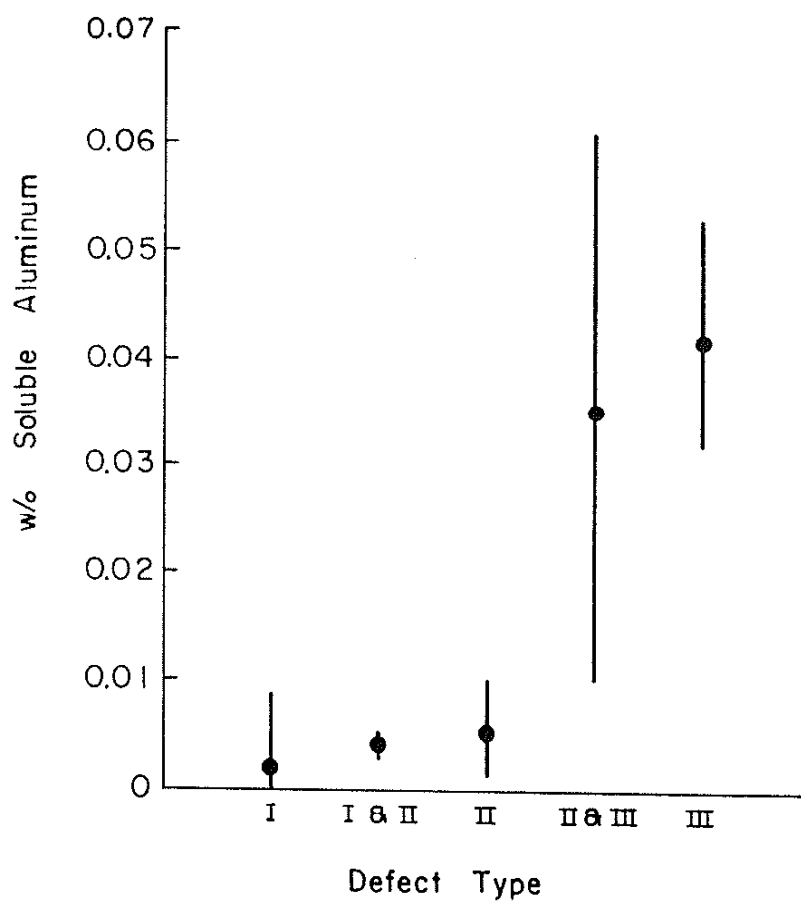


Fig. 5 Type of Inclusions Found in 23 Heats as a Function of Soluble or Residual Al. Content⁽⁵⁾

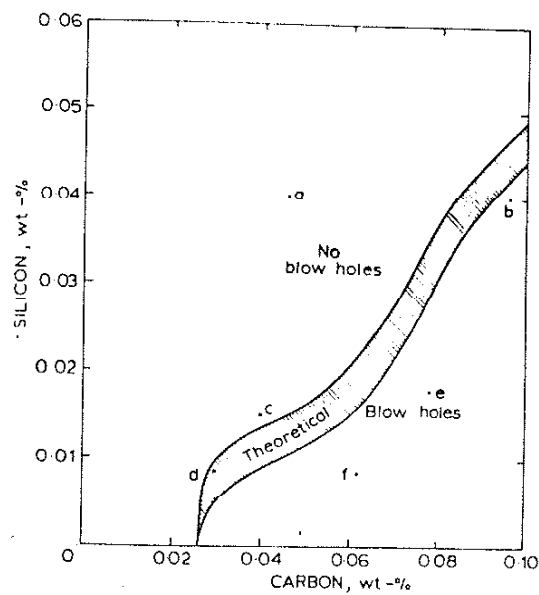
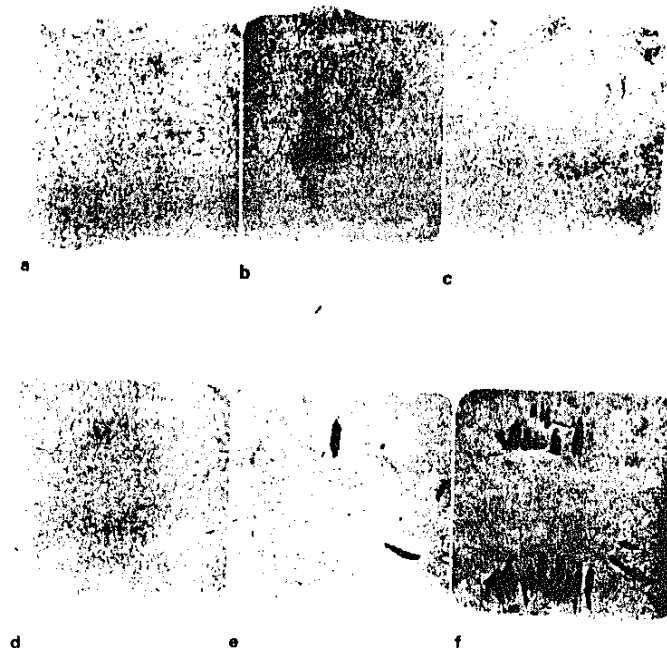


Fig. 6 Critical Amounts of Silicon and Carbon Producing Blowholes in Cast Steels and Unetched Macrosections of Several Ingots⁽¹⁰⁾

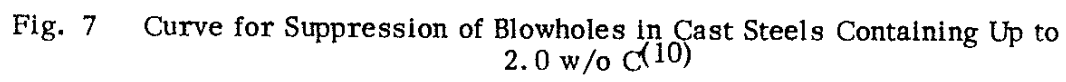


Fig. 7 Curve for Suppression of Blowholes in Cast Steels Containing Up to 2.0 w/o C⁽¹⁰⁾

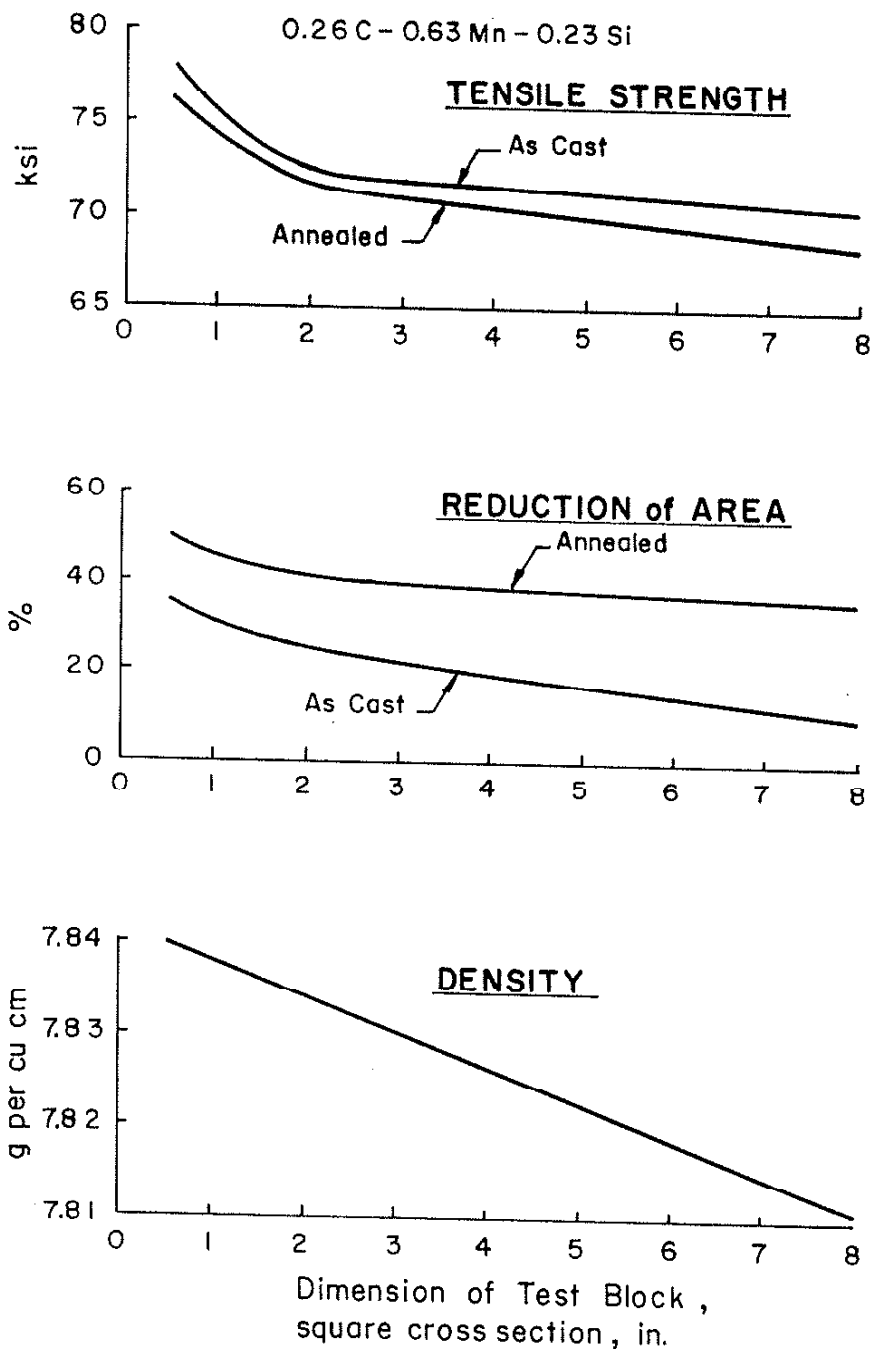
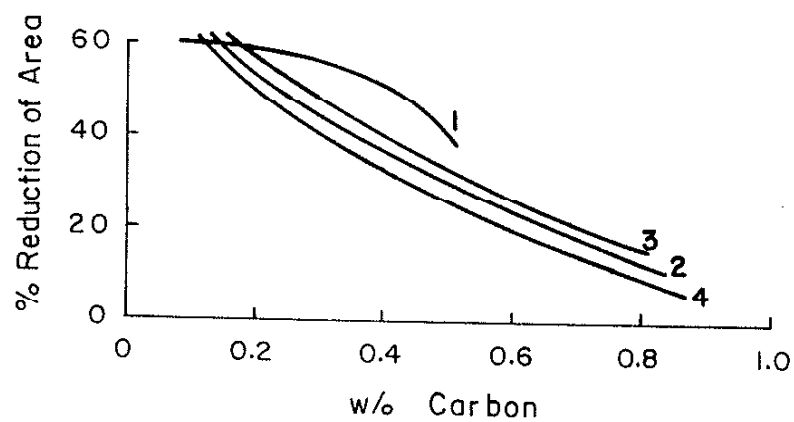
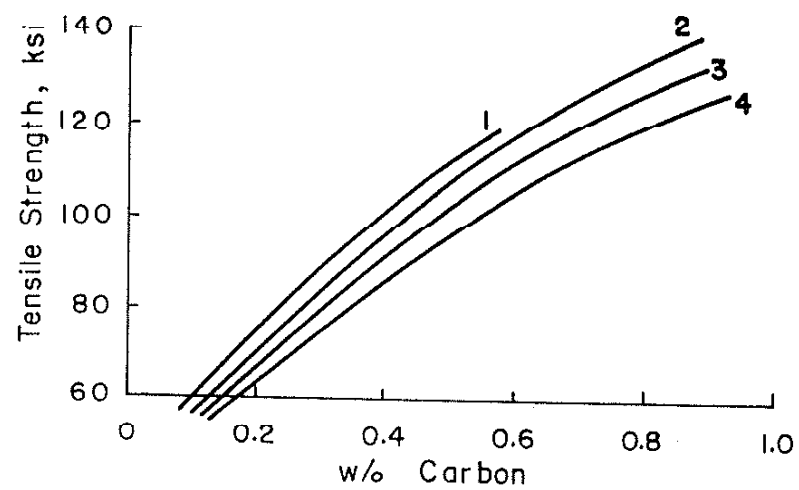


Fig. 8 Decrease in Tensile Strength, Ductility and Density of a Medium Carbon Cast Steel with Increasing Section Size⁽¹²⁾



- 1 - Water quenched & tempered at 1200 F
- 2 - Normalized
- 3 - Normalized & tempered at 1200 F
- 4 - Annealed

Fig. 9 Effect of Carbon Content and Heat Treatment on the Strength and Ductility of Cast Steels⁽¹³⁾

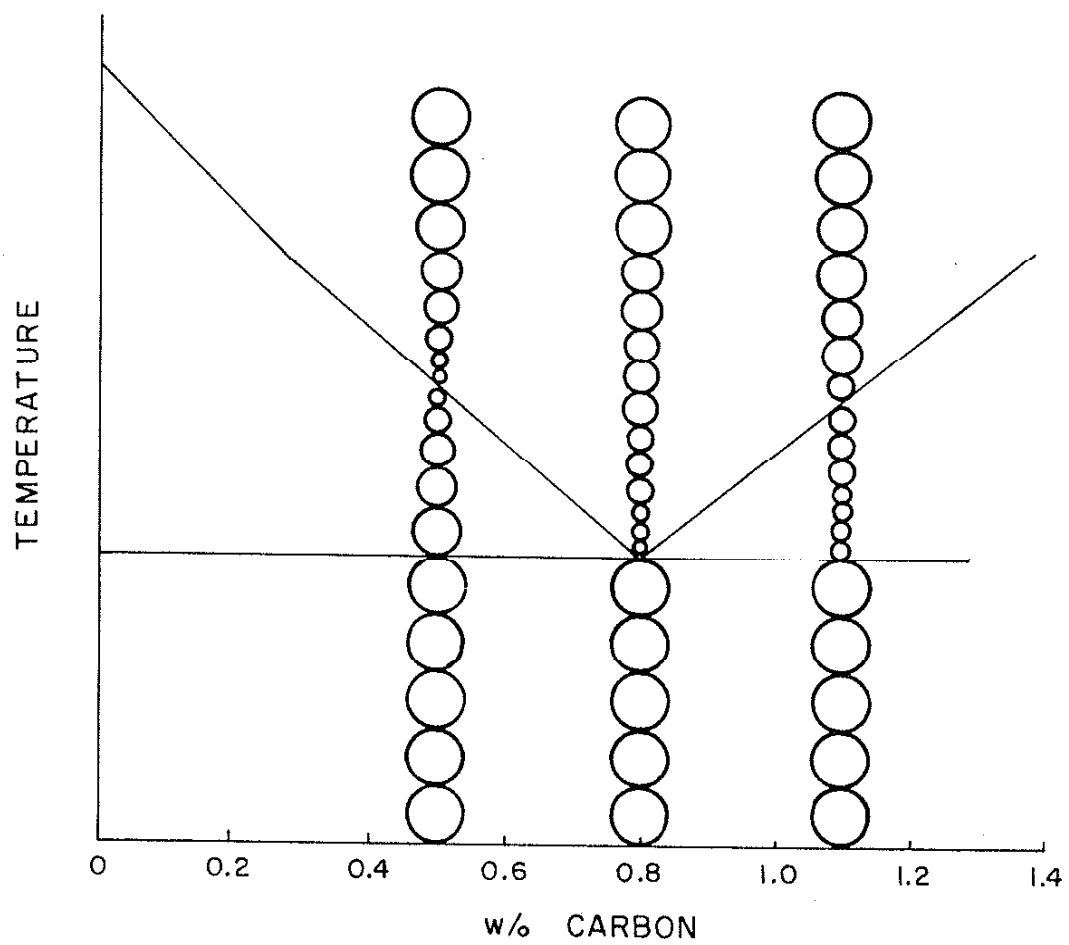


Fig. 10 Schematic of Grain Size Variation as Affected by Heating of Steels

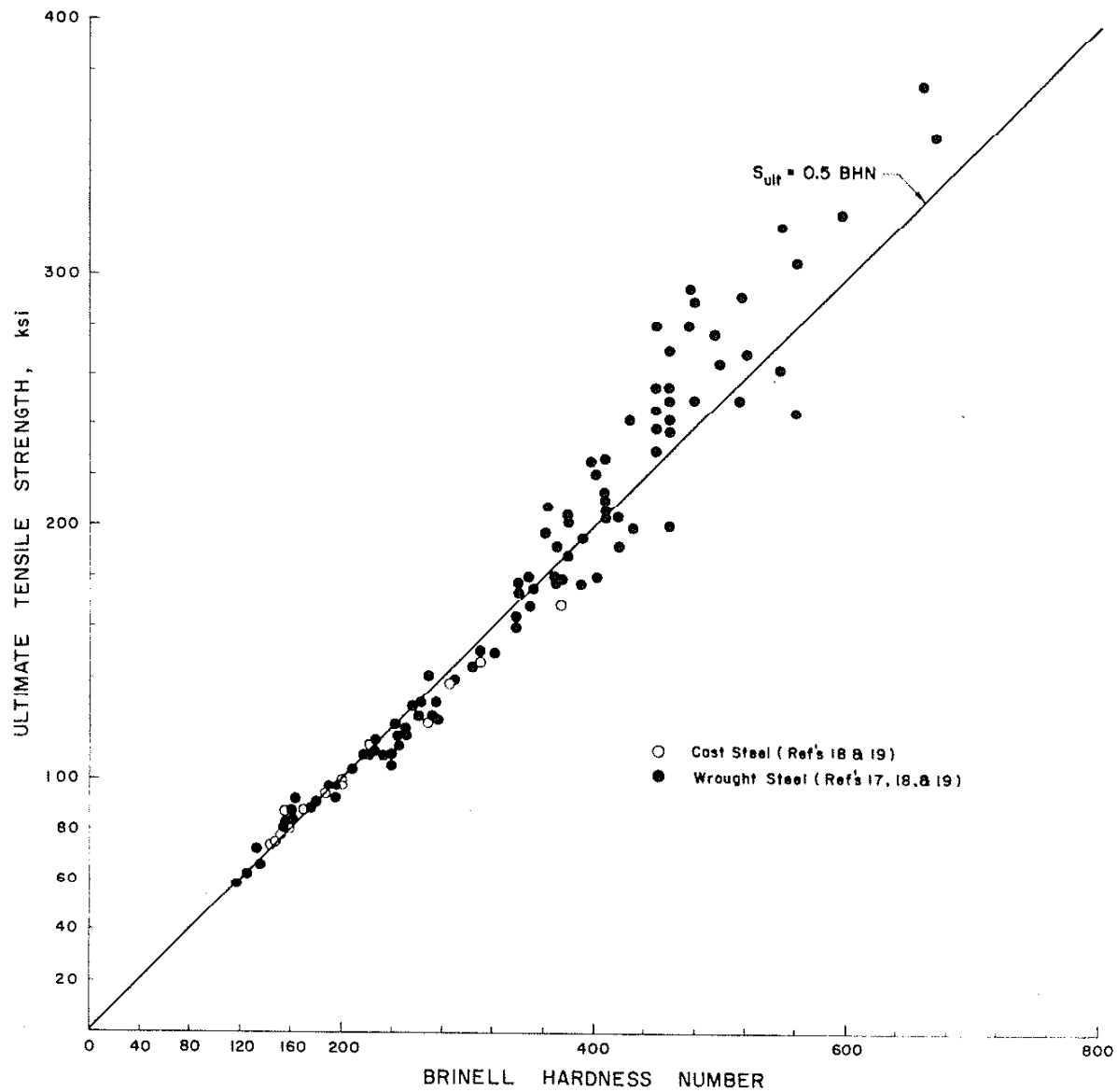


Fig. 11 Ultimate Tensile Strength Vs. Brinell Hardness for Wrought and Cast Steels

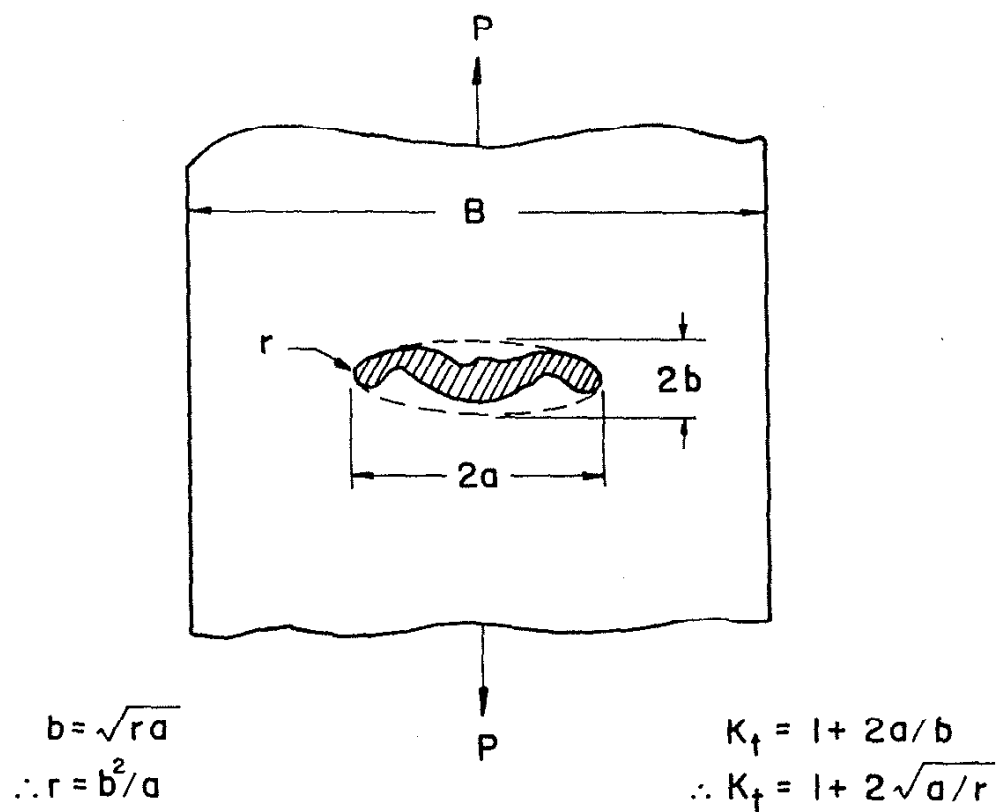


Fig. 12 Approximation of Type II Sulfide Inclusions as Elliptical Flaws in Two Dimensions under Uniaxial Loading⁽²⁵⁾

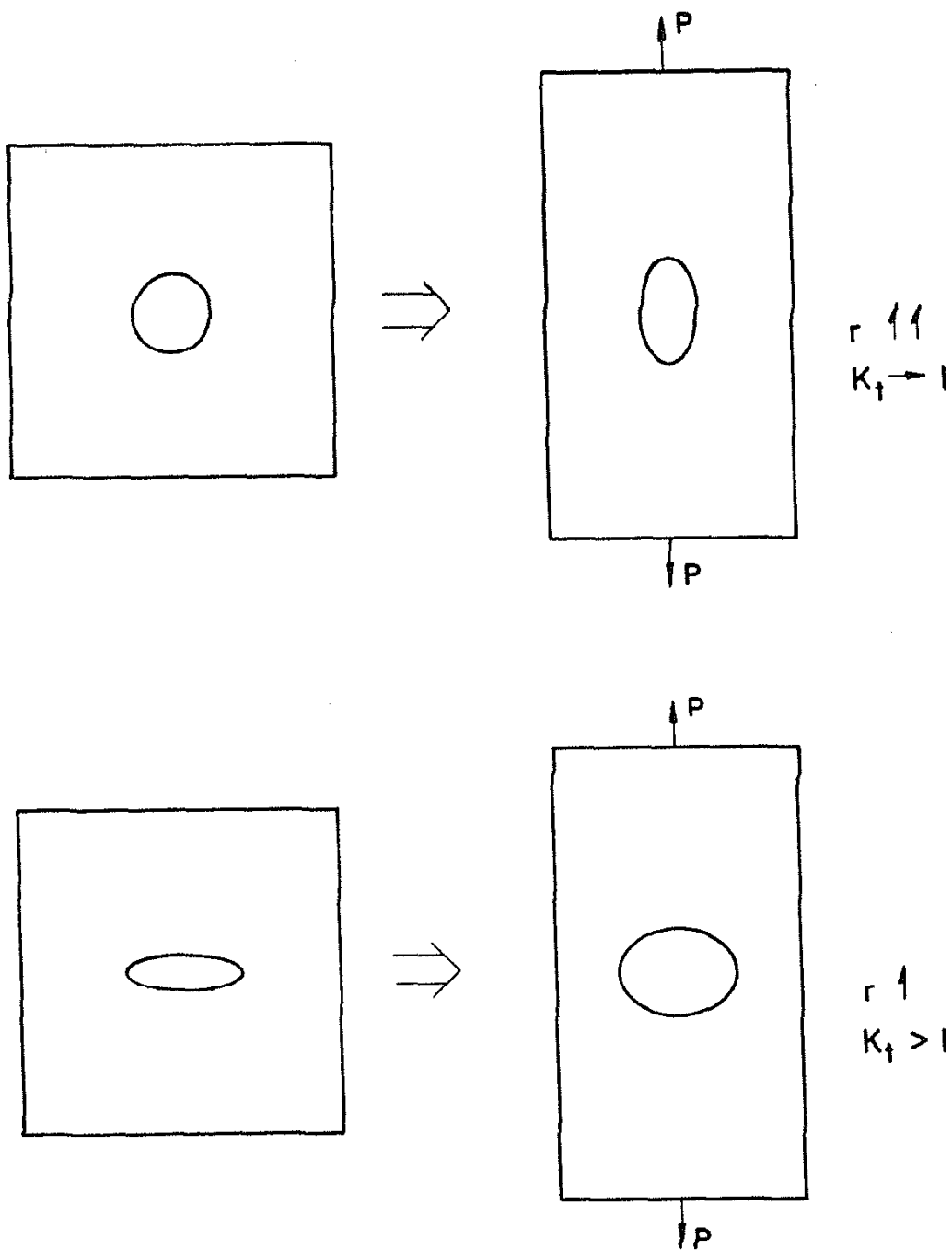


Fig. 13 Schematic of "Plastic Blunting" of a Hole and Ellipse

Izod Impact Strength - Ft. Lbs. Elongation and Reduction of Area - Percent

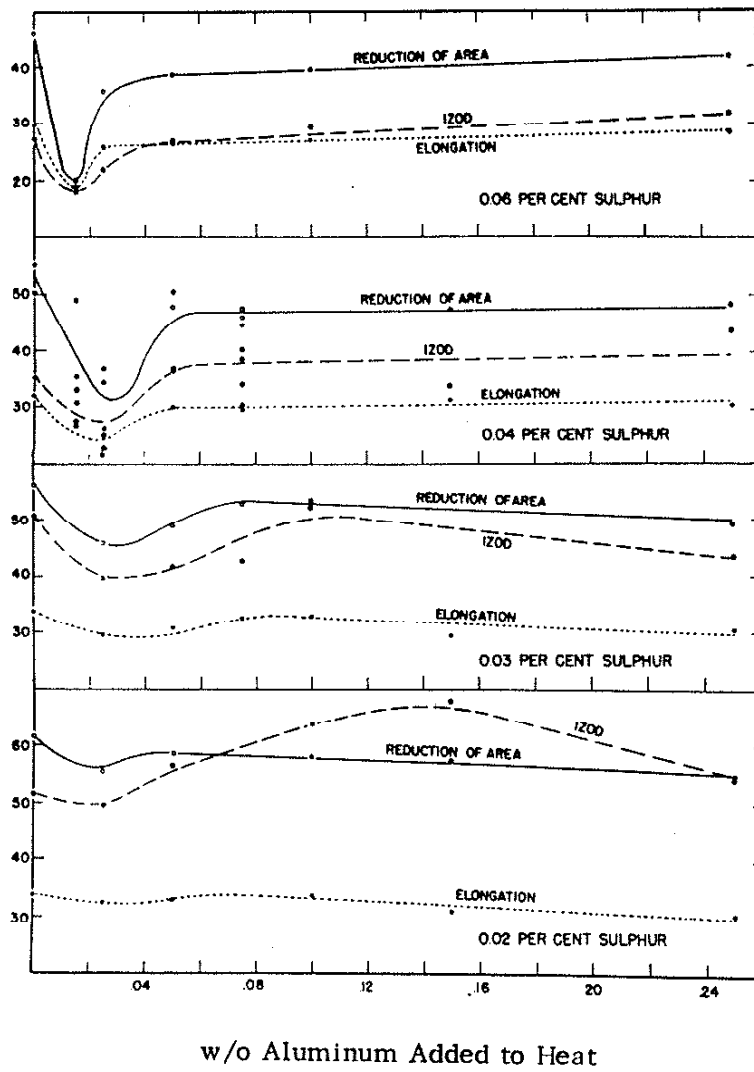


Fig. 14 Effect of Aluminum and Sulfur on the Ductility and Impact Strength of a Medium Carbon Cast Steel⁽⁵⁾

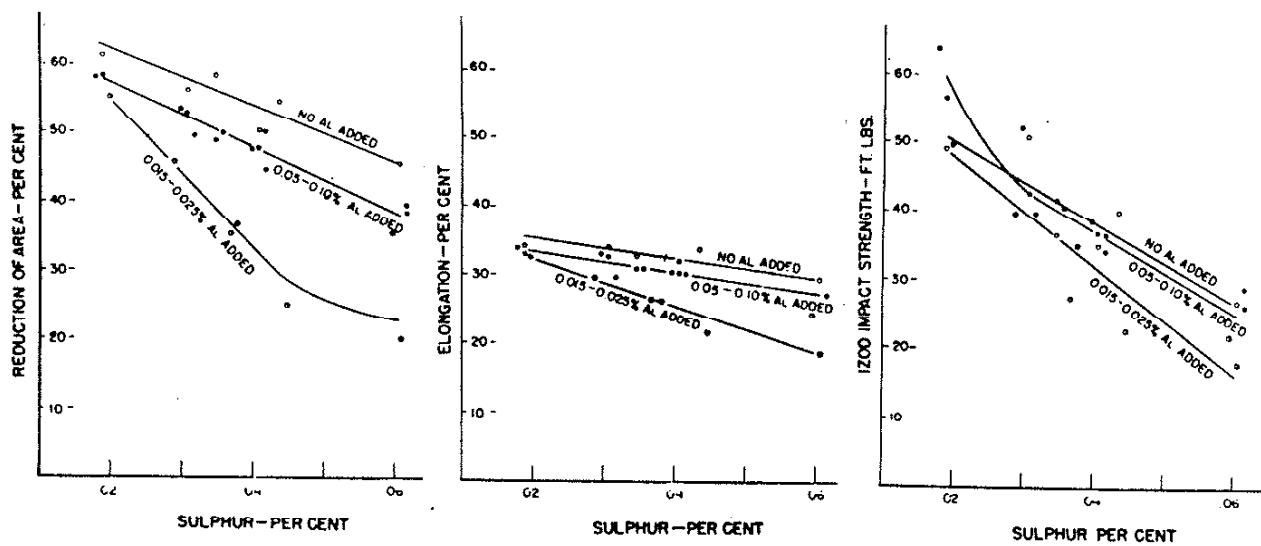


Fig. 15 Effect of Sulfur with and without Aluminum Additions on the Strength and Ductility of a Medium Carbon Cast Steel⁽⁵⁾

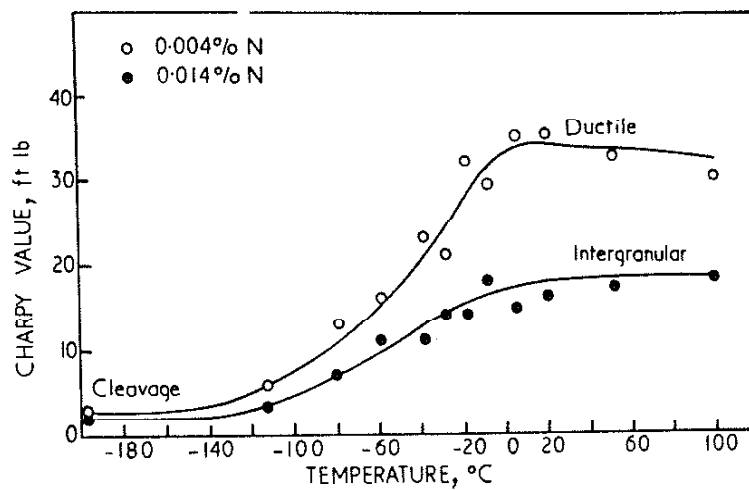


Fig. 16 Variation in Fracture Mode and Impact Strength of a Cast Steel with Differing Nitrogen Content⁽²⁸⁾

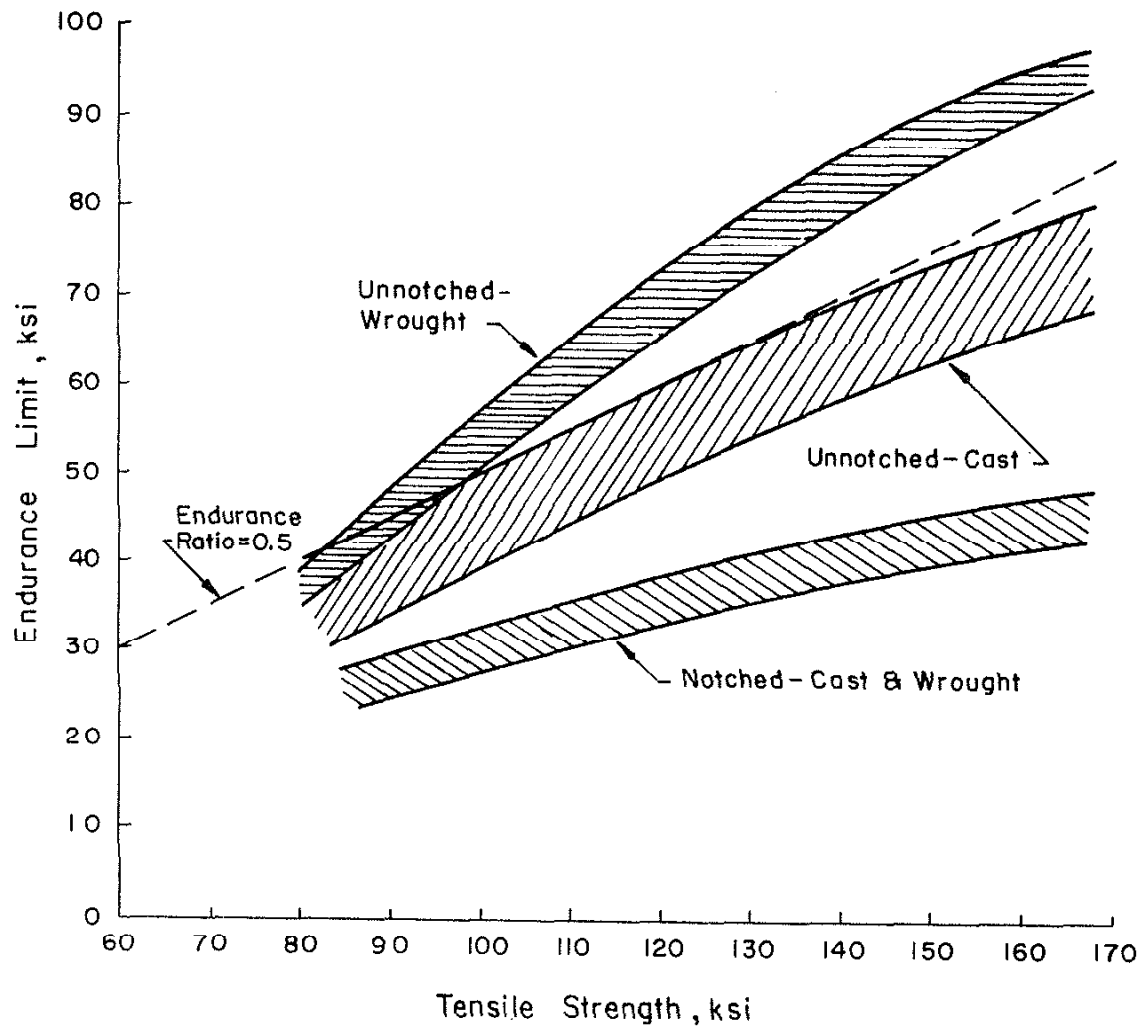


Fig. 17 Ranges of "Endurance Limit" with Tensile Strength for Cast and Wrought Steels⁽¹⁹⁾

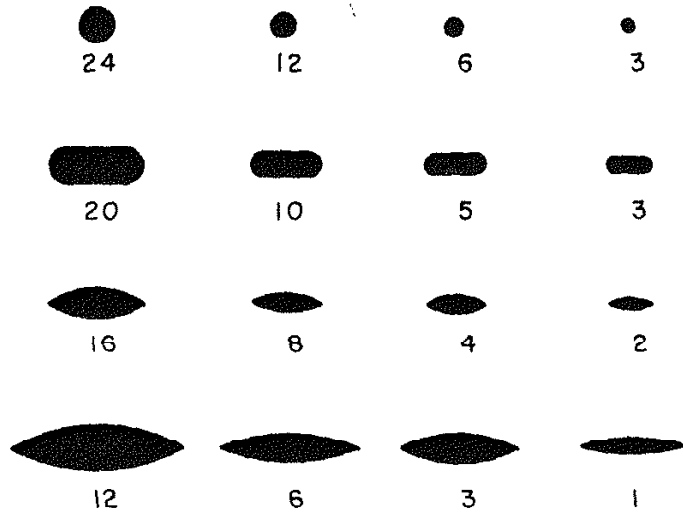


Fig. 18(a) Fairey Count Inclusion Chart Rating Inclusions According to Size and Shape⁽³⁷⁾

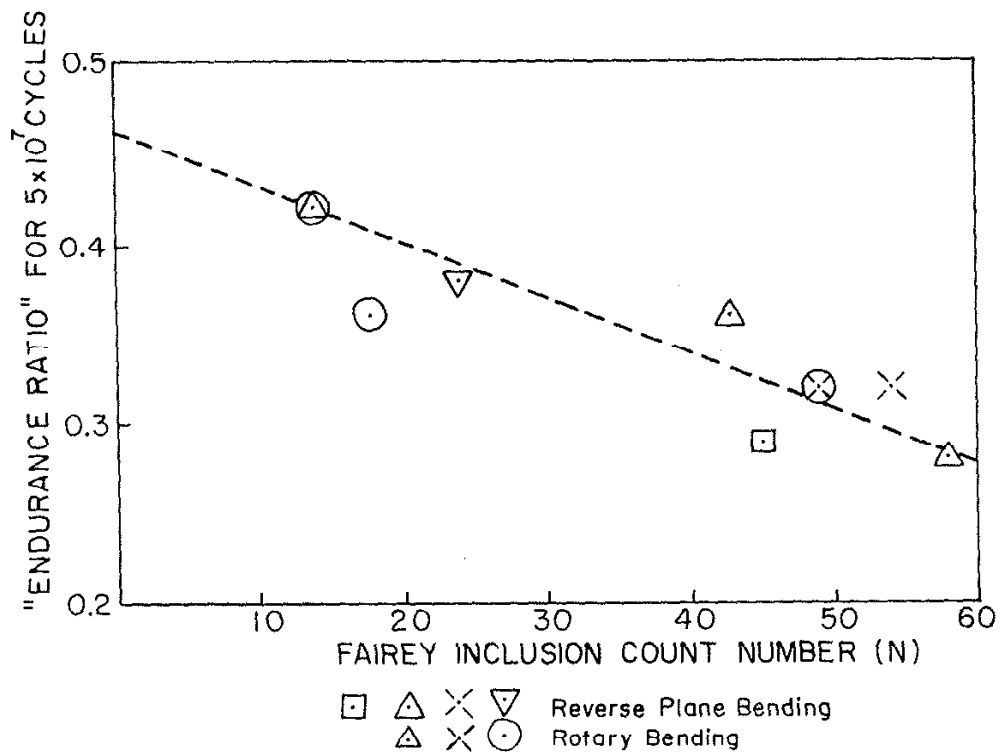


Fig. 18(b) "Endurance Ratio" Vs. Fairey Inclusion Count Number for Various Steels with 125 ksi UTS⁽³⁷⁾

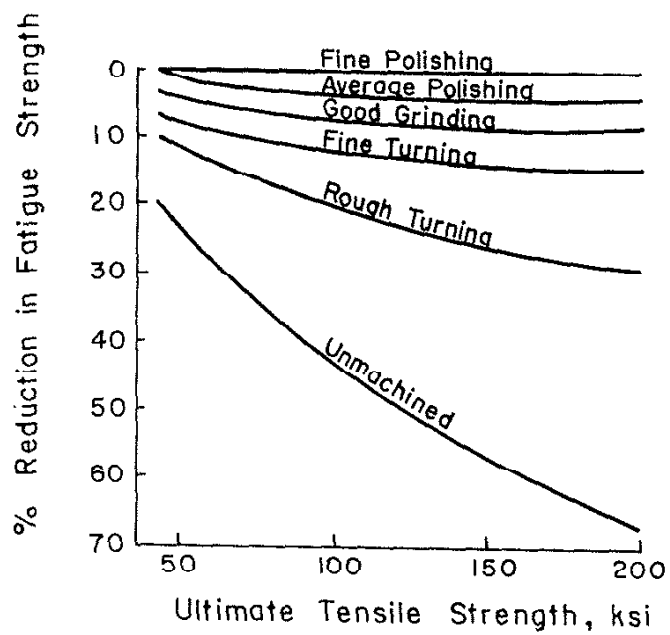


Fig. 19 Reduction in Fatigue Strength of Steels with Varying Surface Finishes and Ultimate Strengths⁽³¹⁾

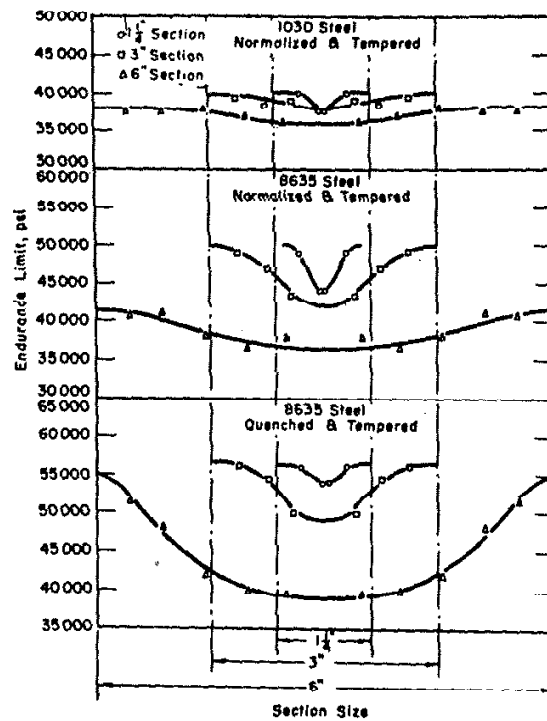


Fig. 20 Distribution of "Endurance Limit" for Cast Steels with Various Section Sizes⁽¹⁹⁾

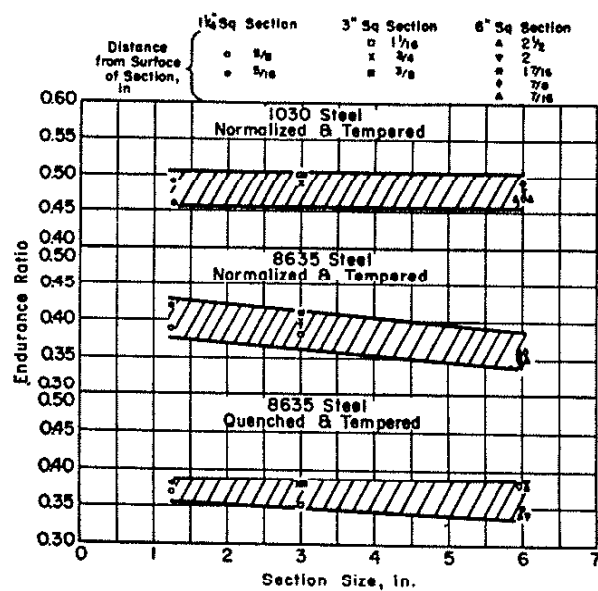


Fig. 21 Ranges of "Endurance Ratios" for Various Section Sizes in Several Cast Steels⁽¹⁹⁾

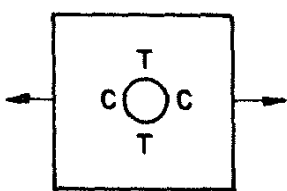
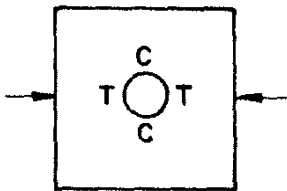
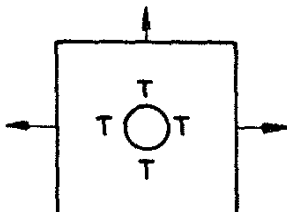
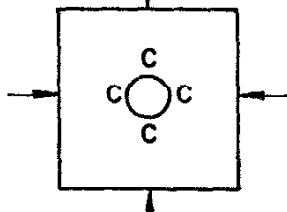
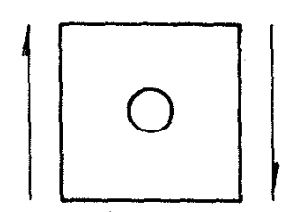
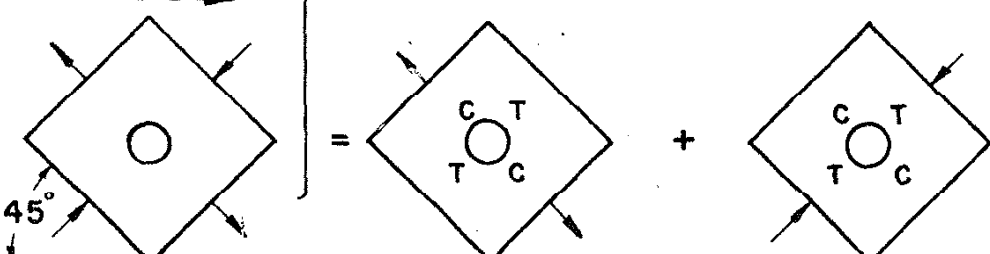
Element	Loading Mode	K_t , Tens. Stress Field	K_t , Comp. Stress Field
	Uniaxial Tension	3	1
	Uniaxial Compression	1	3
	Biaxial Tension	2	0
	Biaxial Compression	0	2
	Torsion	4	4
			

Fig. 22 Effect of Loading Mode on the Theoretical Stress Concentration Factor for a Hole (Two Dimensional)

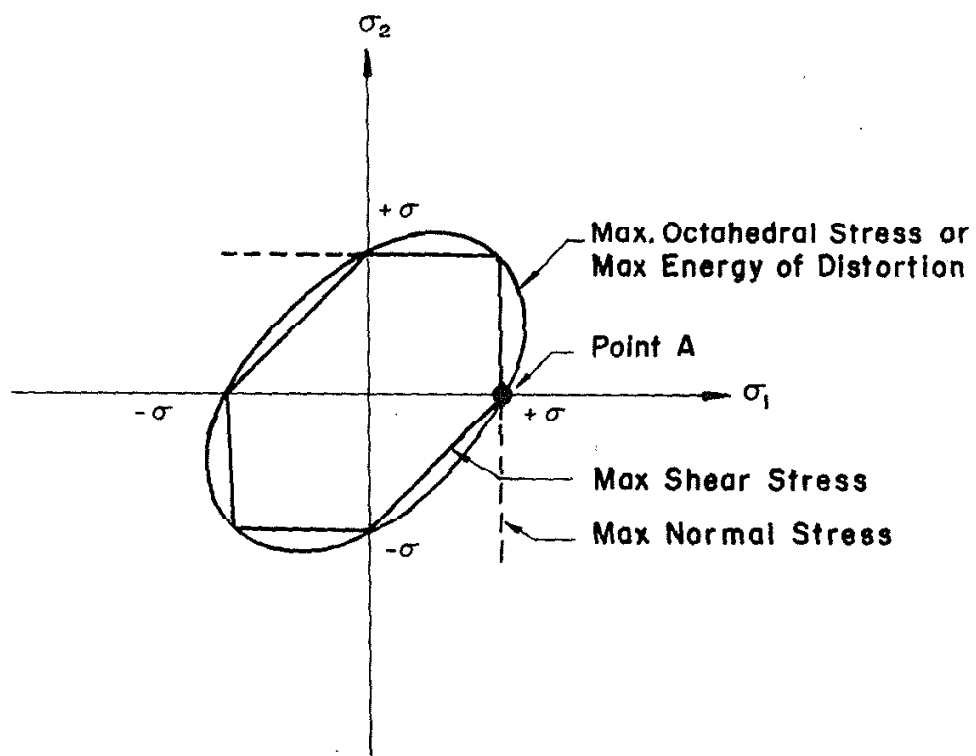
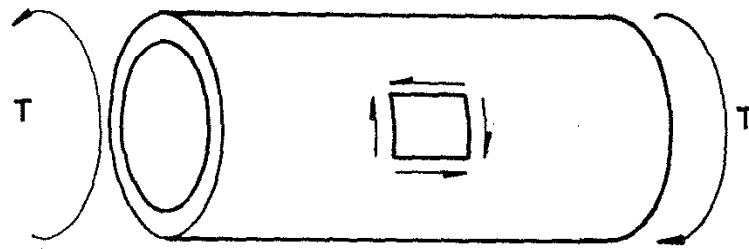
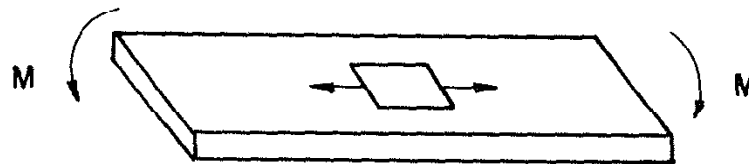


Fig. 23 Yield Criteria for Failure Crossing at a Common Locus on the σ_1 Axis⁽⁴²⁾

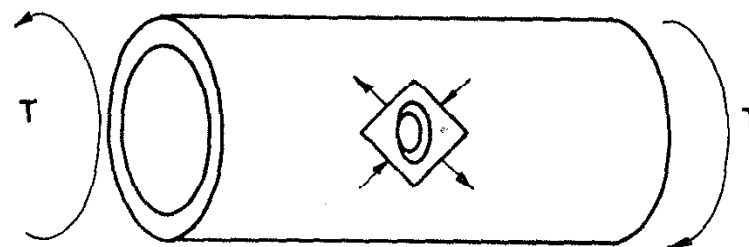
No Stress Concentration



$$\frac{FS_t}{FS_b} = \frac{0.50}{1.00} = 0.577$$

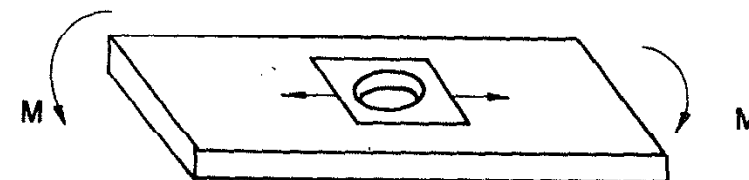


Circular Stress Concentration



$$K_{t_{max}} = 4$$

$$\frac{FS_t}{FS_b} = \frac{3}{4}$$



$$K_{t_{max}} = 3$$

Fig. 24 Schematic of Torsion and Bending of Notched and Unnotched Samples Illustrating the Ratio of Fatigue Strengths

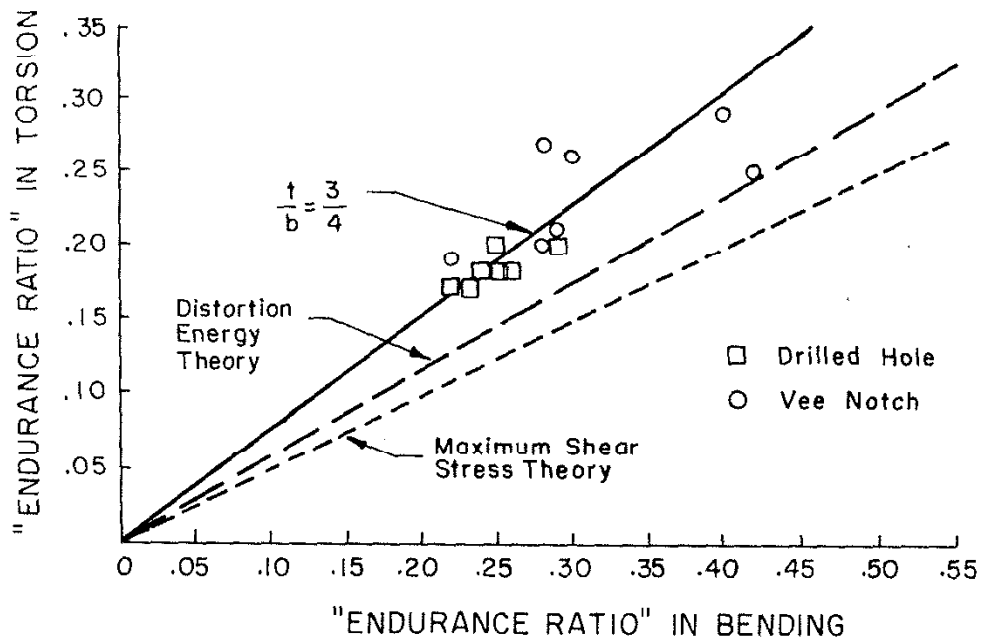


Fig. 25 "Endurance Ratios" in Torsion Vs. Bending⁽³⁵⁾
[Data from Ref. 44]

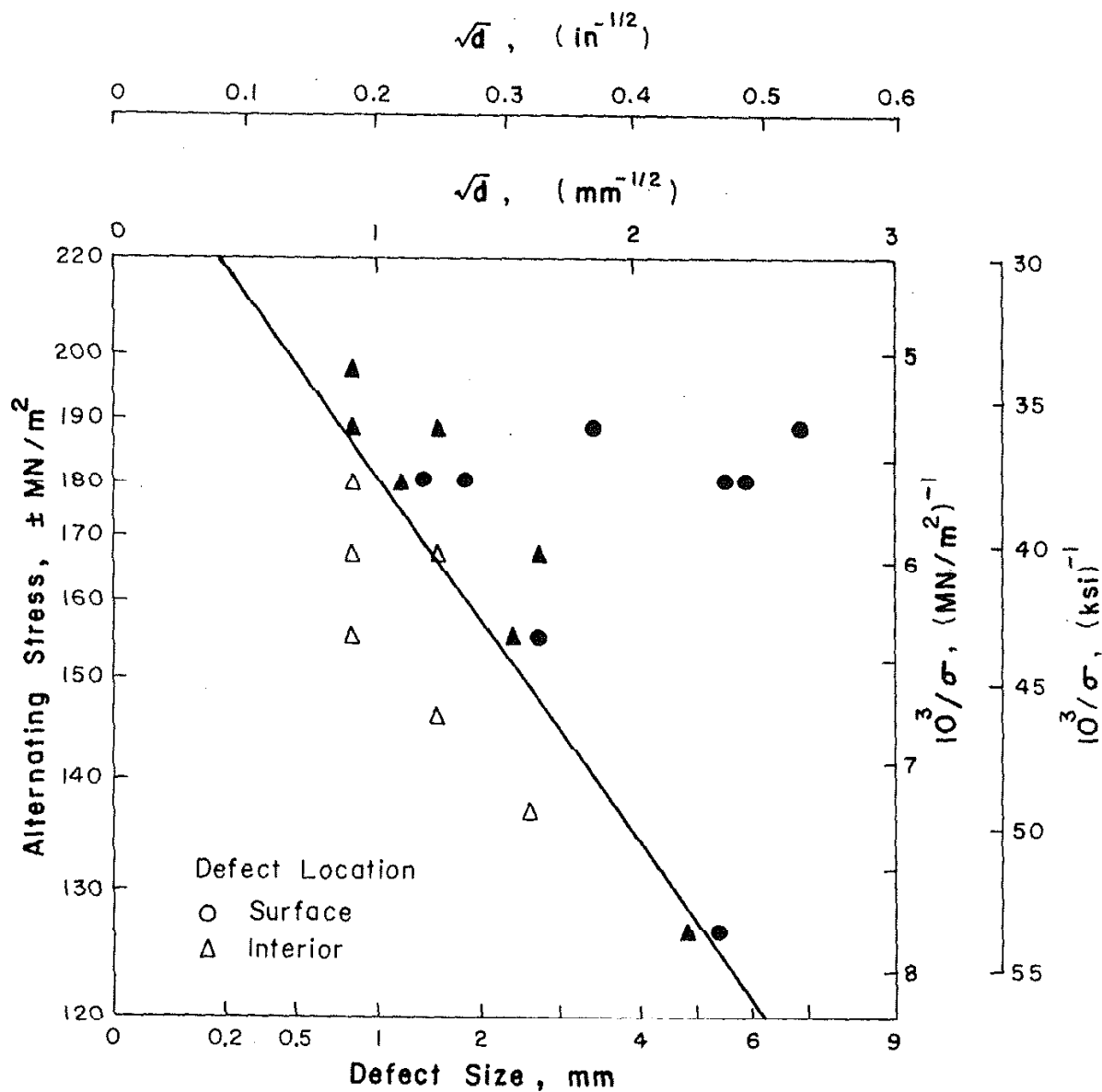
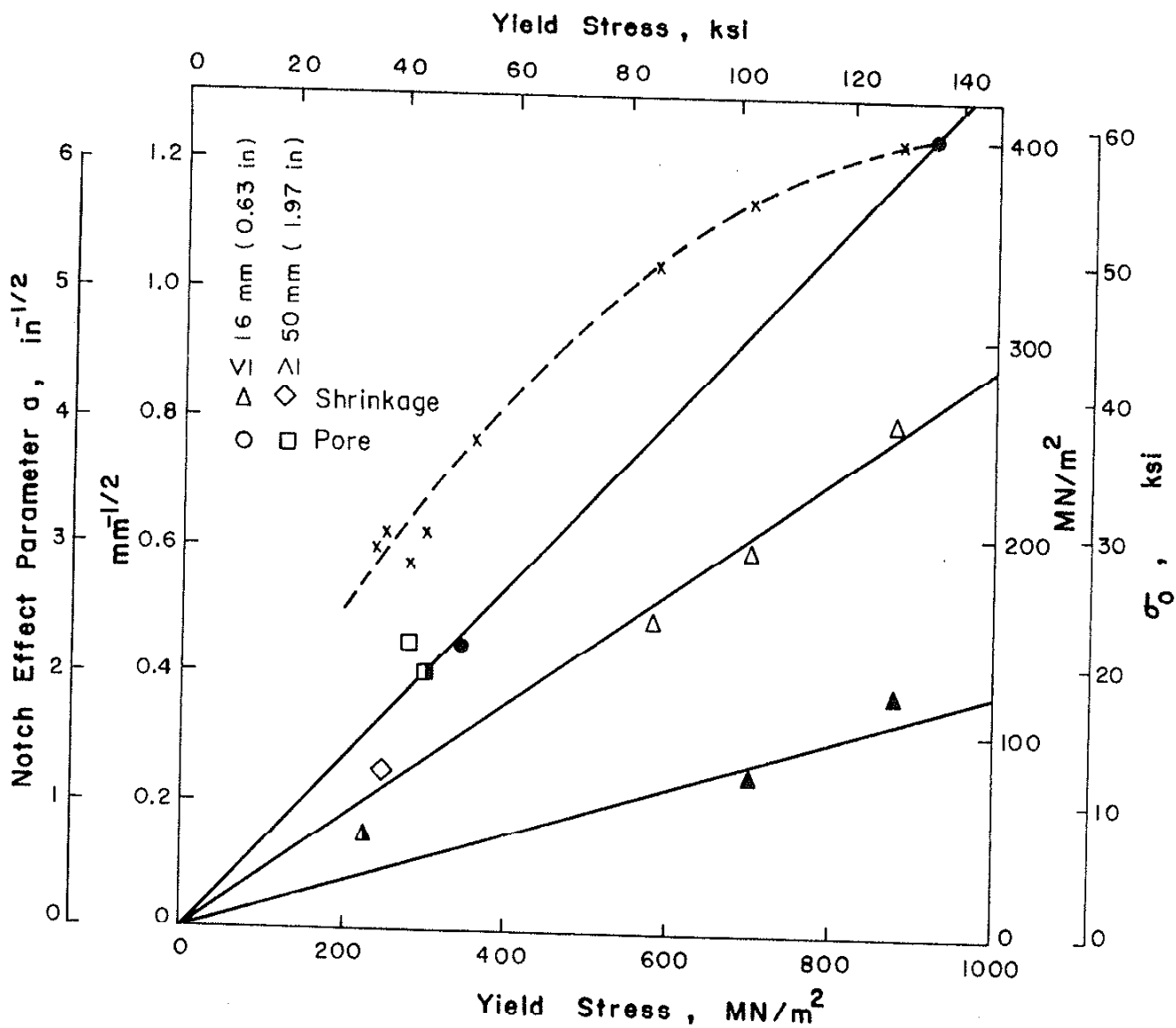


Fig. 26 Alternating Stress of Probit Tests Vs. Defect Size Initiating Failure. Unbroken Specimens are Open Symbols; Broken are Closed Symbols (49)



Defect Location: open symbols = surface
closed symbols = interior

Fig. 27 Notch Effect Parameter, a , and "Defect Free Endurance Limit," σ_0 , Vs. Yield Strength⁽⁴⁹⁾

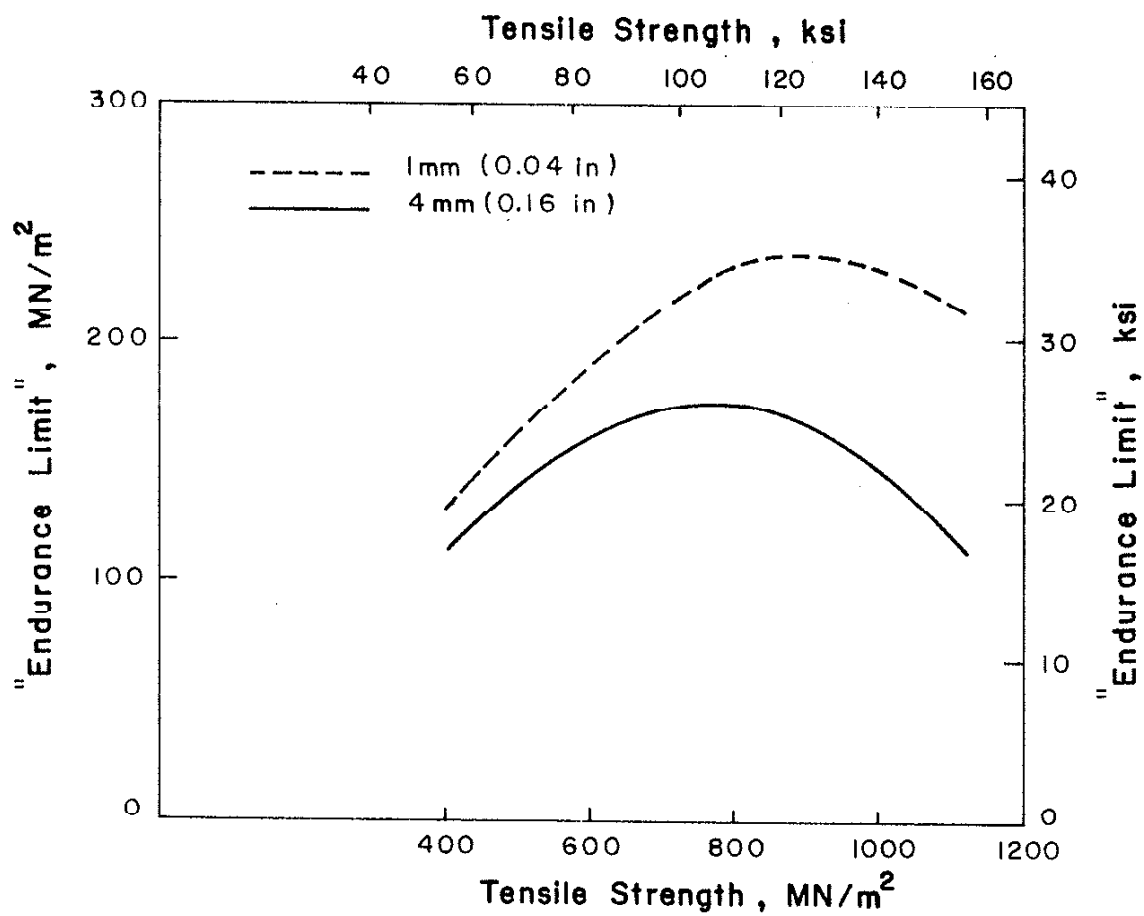


Fig. 28 "Endurance Limit" Vs. Tensile Strength of Cast Steels as a Function of Defect Size Initiating Failure⁽⁴⁹⁾

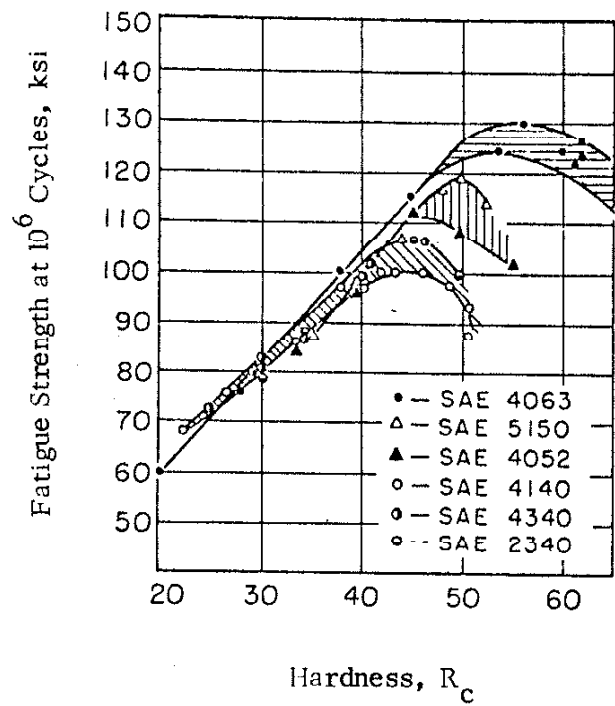


Fig. 29 Fatigue Strength at 10^6 Cycles Vs. Rockwell "C" Hardness of Several Wrought Steels⁽⁶⁴⁾

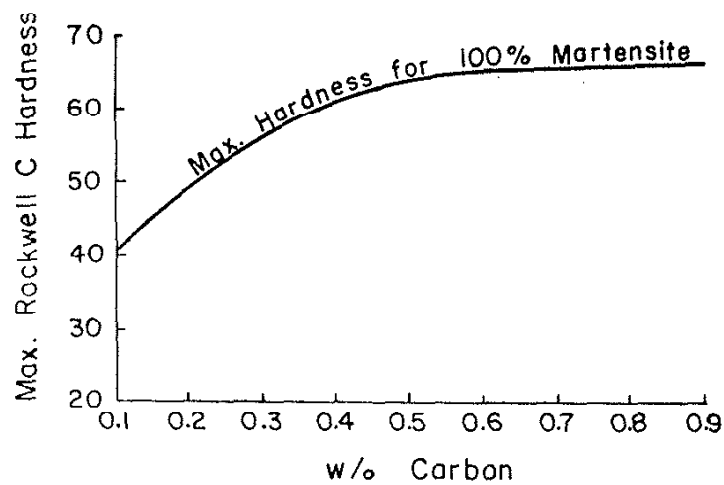


Fig. 30(a) Maximum As-Quenched Hardness Vs. Carbon Content of Steels⁽⁶⁵⁾

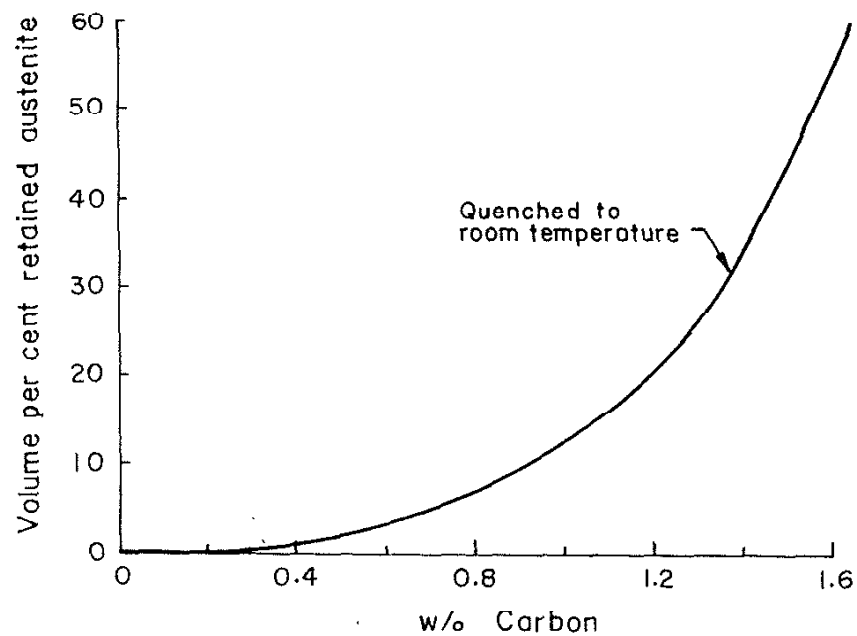


Fig. 30(b) Retained Austenite Vs. Carbon Content of Steels⁽⁶⁶⁾

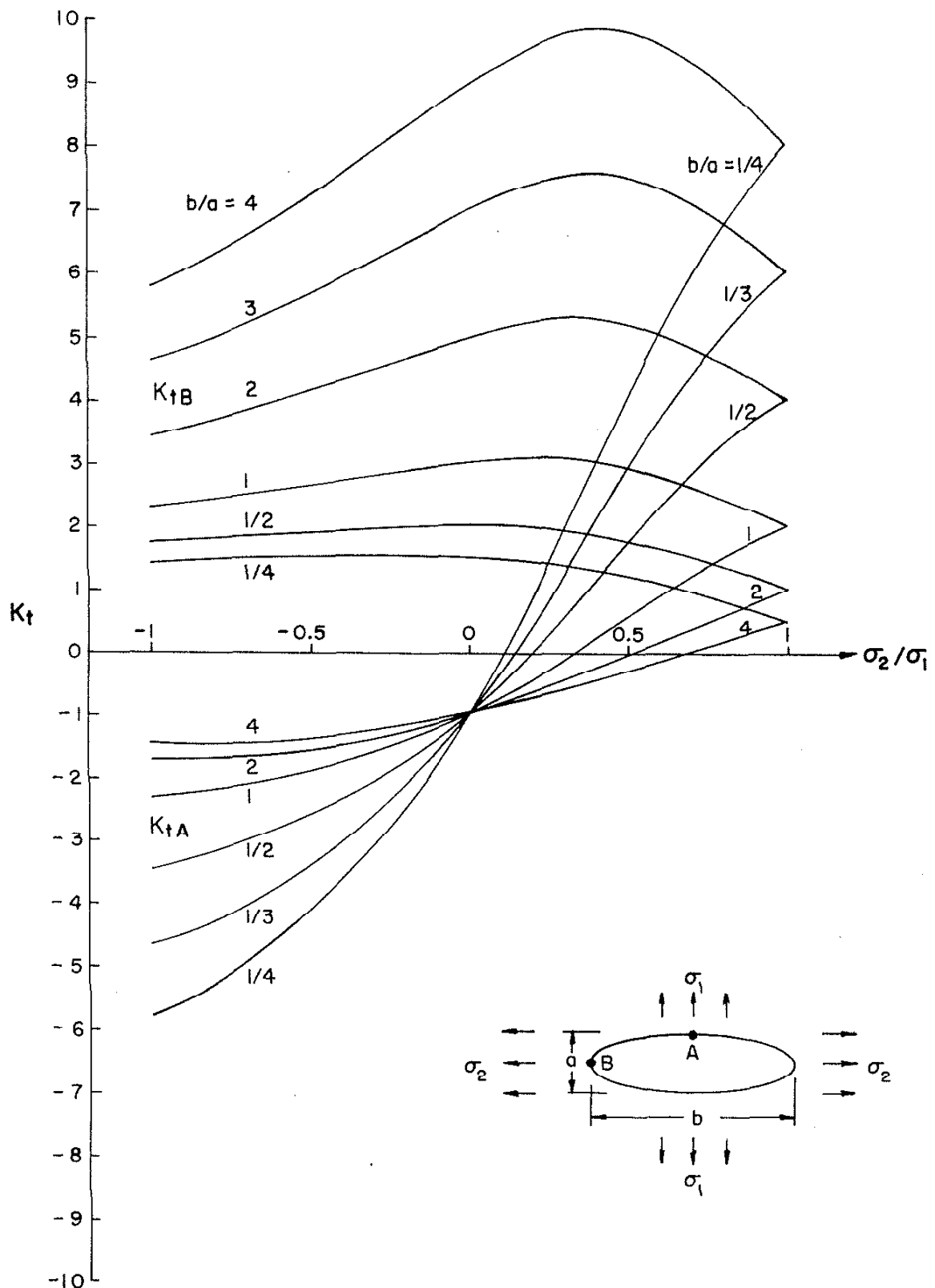


Fig. 31 (a) Theoretical Stress Concentration Factor Vs. Biaxial Stress Ratio for Elliptical Holes⁽⁷¹⁾

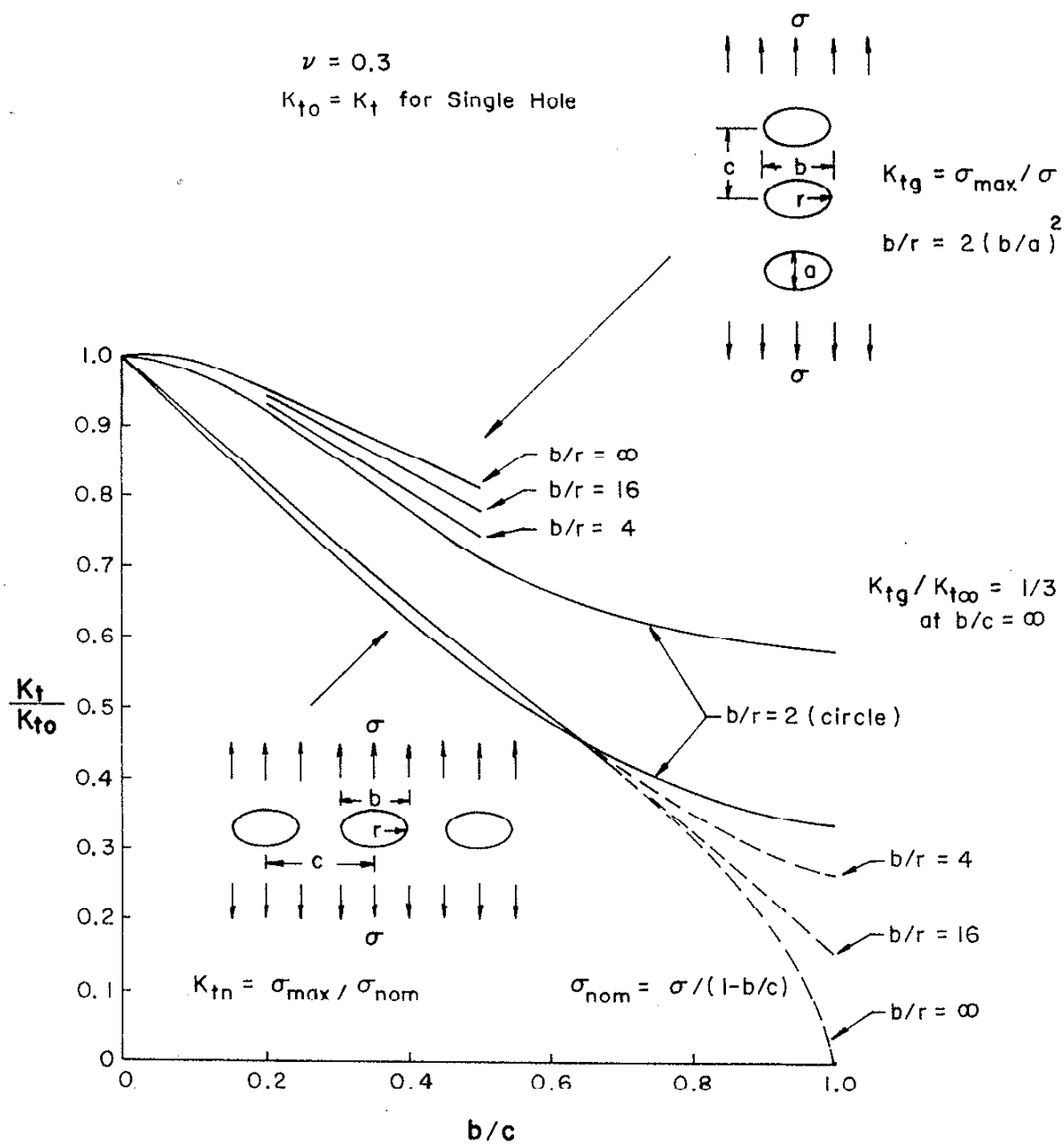


Fig. 31(b) Effect of Spacing on the Theoretical Stress Concentration Factor for a Series of Ellipses Under Uniaxial Tension⁽⁷¹⁾

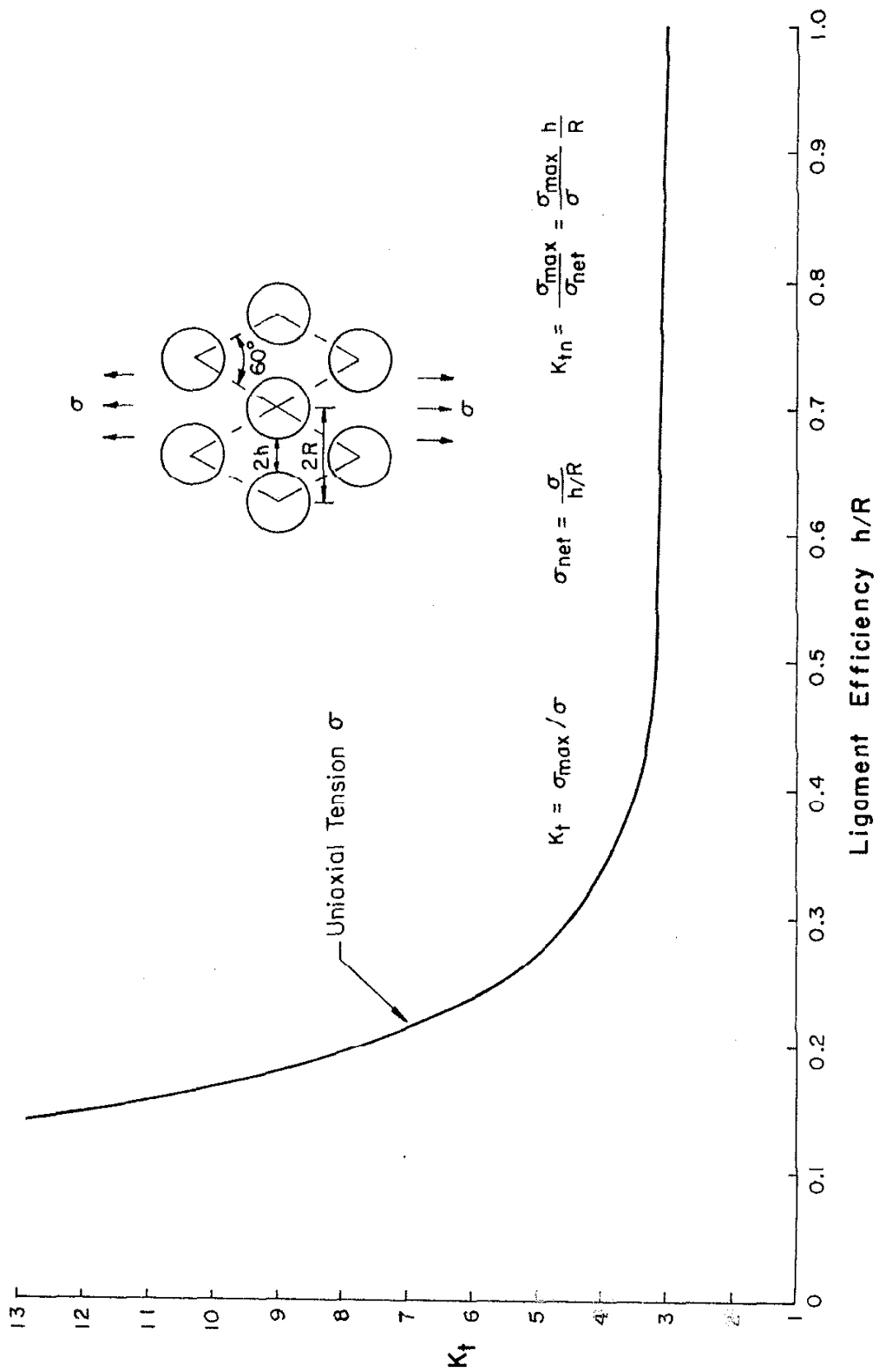


Fig. 31(c) Theoretical Stress Concentration Factor for a Triangular Pattern of Holes⁽⁷¹⁾

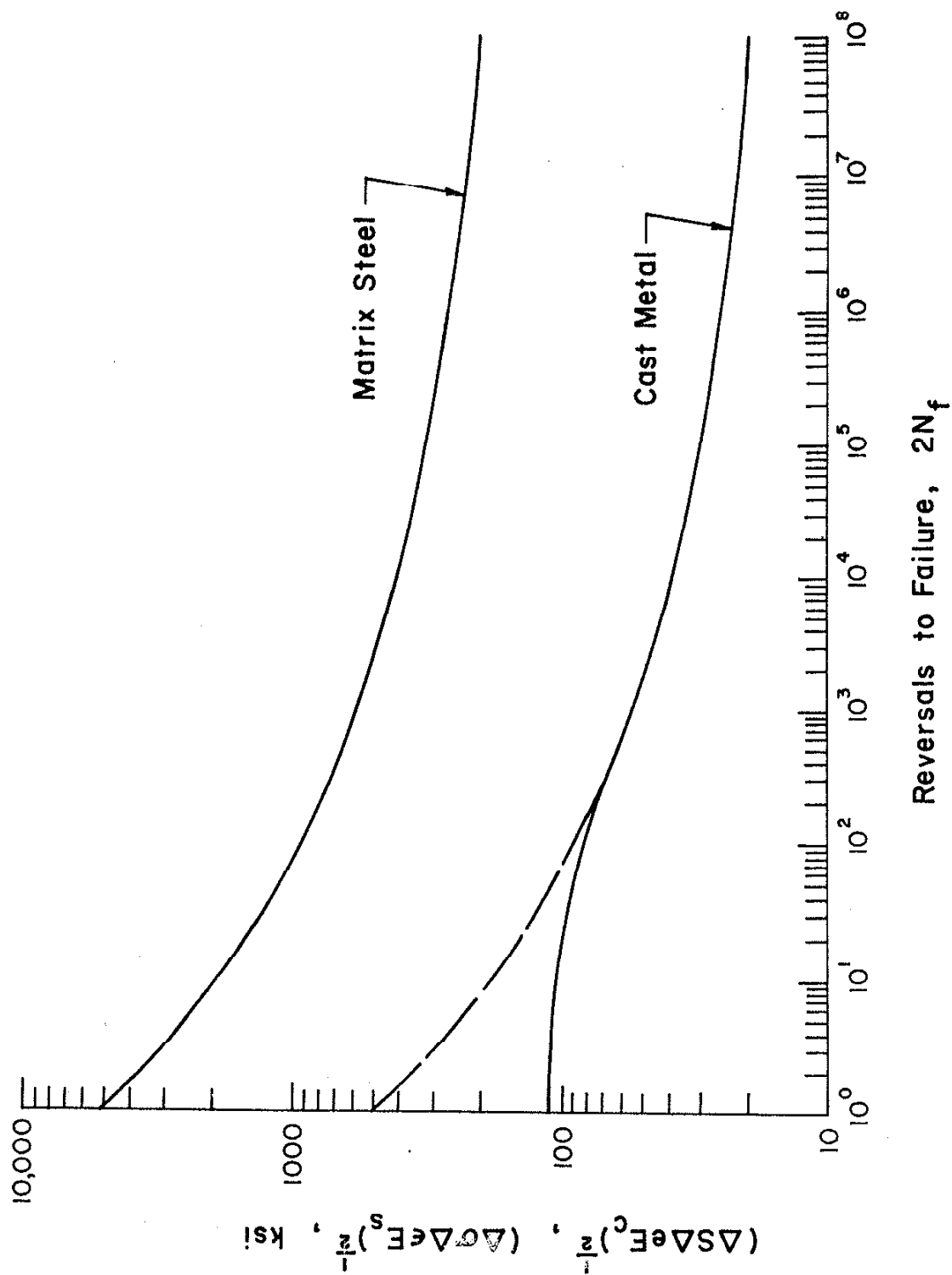


Fig. 32 Neuber Parameter Vs. Reversals to Failure for Matrix Steel and Comparable Cast Alloy